Plasticity Loss in Deep Reinforcement Learning: A Survey

Timo Klein   TIMO.KLEIN@UNIVIE.AC.AT
Faculty of Computer Science
UniVie Doctoral School Computer Science
University of Vienna

Lukas Miklautz   LUKAS.MIKLAUTZ@UNIVIE.AC.AT
Faculty of Computer Science
University of Vienna

Kevin Sidak   KEVIN.SIDAK@UNIVIE.AC.AT
Faculty of Computer Science
UniVie Doctoral School Computer Science
University of Vienna

Claudia Plant   CLAUDIA.PLANT@UNIVIE.AC.AT
Faculty of Computer Science
Research Network Data Science
University of Vienna

Sebastian Tschiatschek   SEBASTIAN.TSCHIATSCHEK@UNIVIE.AC.AT
Faculty of Computer Science
Research Network Data Science
University of Vienna

Abstract

Akin to neuroplasticity in human brains, the plasticity of deep neural networks enables their quick adaption to new data. This makes plasticity particularly crucial for deep Reinforcement Learning (RL) agents: Once plasticity is lost, an agent's performance will inevitably plateau because it cannot improve its policy to account for changes in the data distribution, which are a necessary consequence of its learning process. Thus, developing well-performing and sample-efficient agents hinges on their ability to remain plastic during training. Furthermore, the loss of plasticity can be connected to many other issues plaguing deep RL, such as training instabilities, scaling failures, overestimation bias, and insufficient exploration. With this survey, we aim to provide an overview of the emerging research on plasticity loss for academics and practitioners of deep reinforcement learning. First, we propose a unified definition of plasticity loss based on recent works, relate it to definitions from the literature, and discuss metrics for measuring plasticity loss. Then, we categorize and discuss numerous possible causes of plasticity loss before reviewing currently employed mitigation strategies. Our taxonomy is the first systematic overview of the current state of the field. Lastly, we discuss prevalent issues within the literature, such as a necessity for broader evaluation, and provide recommendations for future research, like gaining a better understanding of an agent's neural activity and behavior.

Keywords: Reinforcement Learning, Plasticity Loss, Continual Learning, Review, Survey

Contents

9 Conclusion **49**

1. Introduction

Deep Reinforcement Learning (RL) has recently seen many successes and breakthroughs: It has beaten the best human players in Go [96] and Dota [11], discovered new matrix multiplication algorithms [30], endows language models with the ability to generate human-like replies for breaking the Turing test [13], and has allowed for substantial progress in robotic control [86]. Its capabilities to react to environmental changes and make near-optimal decisions in challenging sequential decision-making problems are likely crucial for any generally capable agent. Also, RL's mode of learning through interaction purely from trial-and-error mimics human learning, making it a natural paradigm for modeling learning in artificial agents [98].

Despite all the aforementioned successes, deep RL is still in its infancy, and —in many ways— deep RL approaches are not yet reliable and mature. For example, most RL algorithms still use the comparatively small network from the seminal DQN paper [75]. Furthermore, to reach high levels of performance, deep RL typically needs substantial tweaking and elaborate stabilization techniques that are notoriously difficult to get right: From replay buffers and target networks [75] to noise de-correlation [102] and pessimistic value functions [33], and finally to idiosyncratic optimizer settings [4, 66] and bespoke hyperparameter schedules [94].

There are many reasons why this is the case: First and foremost, deep RL is inherently non-stationary, making it a substantially harder learning problem than supervised learning. Additionally, it suffers from its own optimization issues, such as under-exploration, sample correlation, and overestimation bias. Much recent work has been devoted to tackling these problems with ever-more elaborate algorithms, many of them aiming to transfer insights from tabular RL to the deep RL setting [18, 88].

But what if the problems in current deep RL can be attributed to a significant extent to optimization pathologies arising from applying deep neural networks to non-stationary tasks [12, 34, 80]? Recently, this view has gained traction under the umbrella term *plasticity loss*. In the context of deep learning, plasticity refers to a network's ability to quickly adapt to new targets. Consequently, plasticity loss characterizes a network state associated with a lost ability to learn. There is hope and evidence that if the problem of plasticity loss is resolved, this will also alleviate many of the aforementioned RL-specific challenges. The line of work on plasticity loss can be broadly described as trying to find answers to the following two main research questions:

- *Why do the neural networks of deep RL agents lose their learning ability [26, 66, 68, 80, 82, 97]?*

- *How can the ability to learn be maintained [24, 61, 62]?*

These questions are not only relevant for RL but also cover issues relevant to most modern machine learning: They address the fundamental problem of applying machine learning techniques in settings requiring adaptation to changing circumstances. This makes plasticity loss not just relevant for deep RL, but also for other areas applying deep learning, e.g.,

continual learning [26] or the ubiquitous pre-train/fine-tune setup in supervised learning [10, 62].

Scope The focus of this survey is on the phenomenon of plasticity loss in deep RL. As mentioned above, plasticity loss also occurs in continual learning or supervised learning, and while our survey touches on these settings, they are not our focus. Some surveys on continual learning also cover plasticity loss and catastrophic forgetting [104] but do not exclusively focus on plasticity loss—as we do—, thereby naturally limiting the depths of the exposition. Our in-depth focus on plasticity loss also distinguishes our work from Khetarpal et al. [53]'s survey, which discusses several relevant RL-specific sub-areas such as credit assignment or skill learning. In our survey, we emphasize connections between plasticity loss and other issues afflicting deep RL, such as overestimation bias [80] and its inability to scale [29]. Within deep RL, we concentrate on the single-agent setting, as the understanding of plasticity loss is most advanced there.

Structure Our survey starts with an overview of the RL formalism and definitions relevant to plasticity loss in Section 4. As we will see, plasticity loss is intuitively easy to define as networks losing their ability to learn, but there is no single accepted definition in the literature yet. We also use this section to review different experimental setups to test for plasticity loss, including synthetic benchmarks and RL environments. Next, we categorize and present possible hypothesized causes for plasticity loss from the literature in Section 5, followed by a taxonomy of currently deployed remedies (Section 6). Section 7 then discusses some of the factors that deep RL researchers and practitioners should consider when using deep RL algorithms from the perspective of plasticity loss. Finally, our survey concludes with a discussion of the current state of the field and an outlook on future directions in Section 8.

2. Notation and Preliminaries

This section introduces our notation and presents some relevant quantities subsequently used to describe causes and mitigation strategies of plasticity loss. In particular, Section 2.3 presents multiple definitions of a network's feature rank used to measure a representation's quality. These form the basis of multiple regularizes in Section 6.4. In Section 2.4, we also introduce the gradient covariance matrix, which can be used to analyze a network's optimization landscape. Lastly, Section 2.5 reviews synthetic benchmarks and RL environments used to study plasticity loss.

2.1 General Notation

We adopt the following notation: We use lower-case bold symbols for vectors, e.g., $\mathbf{x} \in \mathcal{X} \subseteq \mathbb{R}^{d'}$ to denote an input sample from the data space $\mathcal{X}$ of dimension d'. Upper-case bold symbols denote matrices, e.g., $\mathbf{X} \in \mathbb{R}^{n \times d'}$ denotes the design matrix whose rows contain samples from $\mathcal{X}$. Expectations with respect to a distribution P are denoted as $\mathbb{E}_{\mathbf{a} \sim P}[\cdot]$. If it is clear from the context, we skip the subscript for brevity. We use $\mathrm{SVD}(\mathbf{A})$ to denote the multiset of all singular values of $\mathbf{A}$, σ to denote a single singular value, $\sigma_i(\mathbf{A})$ to denote the ith largest singular value of matrix $\mathbf{A}$ and $\sigma_{\min}$ and $\sigma_{\max}$ to denote the smallest and largest singular value, respectively. For $\phi \colon \mathbb{R}^{d'} \to \mathbb{R}^d$ being a function mapping samples to

features, we denote the feature matrix as $\phi(\mathbf{X}) \in \mathbb{R}^{n \times d}$, where d is the dimension of the representation.

2.2 Reinforcement Learning

Reinforcement learning is concerned with optimizing intelligent agents' actions via trial-and-error to maximize the so-called cumulative reward (defined below). The agents' interactions with an environment are formalized via Markov Decision Processes (MDPs) that can be described as tuples $\mathcal{M} = (\mathcal{S}, \mathcal{A}, \mathcal{P}, r, \rho_0, \gamma)$, where $\mathcal{S}$ is the state space, $\mathcal{A}$ is the action space, i.e., set of possible actions, $\mathcal{P} \colon \mathcal{S} \times \mathcal{S} \times \mathcal{A} \to [0,1]$ is the transition kernel specifying the probability of transitioning from one state to another state upon taking a specific action, $r \colon \mathcal{S} \times \mathcal{A} \to \mathbb{R}$ is the reward function specifying the reward the agent obtains for taking an action in a state, ρ_0 is the initial state distribution, and γ is the so-called discount factor. The behavior of an agent is defined by its possibly stochastic policy $\pi \colon \mathcal{S} \to [0,1]^{|\mathcal{A}|}$ specifying for each state a distribution over the actions the agent can take. We often write $\pi(a|s)$ to denote the probability of action a in state s according to policy π. The agent aims to maximize the (discounted) cumulative reward

$$J(\pi) = \mathbb{E}\left[\sum_{t=0}^{\infty} \gamma^t r(s_t, a_t) \mid \pi\right], \tag{1}$$

where the expectation is over the randomness of the transitions, the agent's policy, and the initial state. An optimal policy π^* maximizes $J(\pi)$.

Key quantities for RL algorithms are the *state-value*,

$$V^\pi(s) = \mathbb{E}\left[\sum_{t=0}^{\infty} \gamma^t r(s_t, a_t) \mid s_0 = s\right], \tag{2}$$

i.e., the expected cumulative reward when starting from state s and following policy π from there, and the *action-value*,

$$Q^\pi(s, a) = \mathbb{E}\left[\sum_{t=0}^{\infty} \gamma^t r(s_t, a_t) \mid s_0 = s, a_0 = a\right], \tag{3}$$

i.e., the expected return starting from state s, taking action a, and following policy π afterwards. An optimal policy can be found by maximizing the expected value of the initial state, i.e.,

$$\pi^* \in \arg\max_\pi \mathbb{E}_{s \sim \rho_0}[V^\pi(s)] \tag{4}$$

Note that state-values (and, similarly, action-values) can also be defined recursively:

$$V^\pi(s) = \mathbb{E}_{a \sim \pi(s)}[r(s, a) + \gamma \sum_{s'} \mathcal{P}(s, s', a) V^\pi(s')], \tag{5}$$

Inspired by these recursive definitions are so-called *temporal-difference* learning approaches, e.g., approaches based on iteratively updating state-value estimates as

$$V^\pi(s_t) \leftarrow V^\pi(s_t) + \alpha \underbrace{[r_{t+1} + \gamma V^\pi(s_{t+1}) - V^\pi(s_t)]}_{\text{TD error}}. \tag{6}$$

In these approaches, estimates of state-values (or action-values) are updated based on estimates of those values for successor states (and actions) — that is why such methods are also called *bootstrapping methods*. The term within brackets is also referred to as *TD error*.

In deep RL agents, V^π, Q^π or π (or combinations of those) are represented by deep neural networks. Many works [42, 64] decompose a deep RL agent into a learned representation ϕ, covering all layers up to and including the penultimate layer, and a linear transformation $\mathbf{W}$. This allows viewing an RL agent's policy or value function as a linear function of some learned non-linear features, i.e., features obtained through a non-linear transformation of the states $\phi(s)$ or corresponding observations. Using the value function as an example, our notation for this decomposition is $V(s) = \langle \phi(s), \mathbf{W} \rangle$.

2.3 Definitions of Effective Rank

The effective rank is a measure commonly used to assess the quality of the representation learned by a neural network [46, 56, 67]. To build an intuition of why the effective rank matters, recall the computation of of an RL agent's value function as $V(s) = \langle \phi(s), \mathbf{W} \rangle$, i.e., as the inner product of non-linear features of the state and weights $\mathbf{W}$. Now suppose that $\phi(s) \in \mathbb{R}^d$ is low rank: This implies that the network's features lie in a lower dimensional subspace of $\mathbb{R}^d$, potentially mapping dissimilar states to similar feature vectors, which in turn makes it harder to learn distinct values for these dissimilar states [71]. For a full-rank $\phi(s)$, the network maps different states to dissimilar feature vectors by distributing them along all directions of $\mathbb{R}^d$, facilitating easier learning of distinct values for different states.

Multiple possible definitions of the effective rank have been considered in the literature, some of which we review here. The effective rank definition below is based on the *energy ratio* (also called *cumulative explained variance*) commonly used in principal component analysis and defined as the minimum k such that a rank-k approximation of the feature matrix explains a $(1 - \delta)$ fraction of its total variance.

Definition 1 (Effective Rank [56]) *Let $\phi \colon \mathcal{X} \to \mathbb{R}^d$ be a feature mapping and $\phi(\mathbf{X}) \in \mathbb{R}^{n \times d}$ be a feature matrix, e.g., the embeddings of a neural network for a collection of samples $\mathbf{X}$. Let $\delta \in [0, 1]$ and $\sigma_1 \geq \cdots \geq \sigma_d \geq 0$ be the singular values of $\phi(\mathbf{X})$ in increasing order. The* effective rank *is defined as*

$$\mathrm{srank}_\delta(\phi(\mathbf{X})) = \min \left\{ k : \frac{\sum_{i=1}^k \sigma_i(\phi(\mathbf{X}))}{\sum_{i=1}^d \sigma_i(\phi(\mathbf{X}))} \geq 1 - \delta \right\}. \tag{7}$$

The *feature rank* defined below can be understood as quantifying "how easily states can be distinguished by updating only the final layer of the network" [65], given by the feature mapping ϕ. The feature rank (cf. Section 4) was introduced to approximate the *target fitting capacity* while being cheaper to compute.

Definition 2 (Feature rank [65]) *Let $\phi \colon \mathcal{X} \to \mathbb{R}^d$ be a feature mapping. Let $\mathbf{X}_n \subset \mathcal{X}$ be a set of n states in $\mathcal{X}$ sampled from some fixed distribution P. Fix $\varepsilon \geq 0$, and let $\phi(\mathbf{X}_n) \in \mathbb{R}^{n \times d}$ denote the feature matrix whose rows are the feature embeddings of states $x \in \mathbf{X}_n$. The* feature rank *of ϕ for distribution P is defined as*

$$\rho(\phi, P, \epsilon) = \lim_{n \to \infty} \mathbb{E}_{\mathbf{X}_n \sim P} \left[\left| \left\{ \sigma \in \mathrm{SVD} \left(\frac{1}{\sqrt{n}} \phi(\mathbf{X}_n) \right) \middle| \sigma > \varepsilon \right\} \right| \right]. \tag{8}$$

> **Feature Rank Definitions**
>
> - Kumar et al. [56] provide the most widely used definition of feature rank, using the sorted singular values $\sigma_1(\phi) \geq \sigma_2(\phi) \geq \ldots$ of an agent's penultimate layer representation ϕ:
>
> $$\mathrm{srank}_\delta(\phi, \mathbf{X}) := \min \left\{ k : \frac{\sum_{i=1}^k \sigma_i\big(\phi(\mathbf{X})\big)}{\sum_{i=1}^d \sigma_i\big(\phi(\mathbf{X})\big)} \geq 1 - \delta \right\},$$
>
> where δ is a threshold parameter usually set to $\delta = 0.01$.
>
> - Lyle et al. [65] define the feature rank as the number of singular values of the (normalized) feature matrix exceeding a specified threshold:
>
> $$\mathrm{srank}_\epsilon(\phi, \mathbf{X}) = \left| \left\{ \sigma \in \mathrm{SVD}\left(\frac{1}{\sqrt{n}} \phi(\mathbf{X}) \right) \middle| \sigma > \varepsilon \right\} \right|,$$
>
> with ϵ being a threshold parameter set to $\epsilon = 0.01$.
>
> - In supervised learning, a definition based on the entropy of the distribution of normalized singular values has started to gain traction [46]. This has the advantage of not requiring a threshold parameter and being continuous:
>
> $$\mathrm{srank}_{\mathrm{continuous}}(\phi, \mathbf{X}) = - \sum_{i=1}^{\min(n,m)} \bar{\sigma}_i\big(\phi(\mathbf{X})\big) \, \log\big(\bar{\sigma}_i\big(\phi(\mathbf{X})\big)\big),$$
>
> where $\bar{\sigma}_i = \sigma_i / \sum_i \sigma_i = 1$.

2.4 Gradient Covariance Matrix and Empirical Neural Tangent Kernel

The gradient covariance matrix and empirical neural tangent kernel (eNTK) are closely related quantities, giving insights into the optimization behavior and the generalization abilities of a neural network [66] by analyzing the dot product of the gradients of different samples $\mathbf{x}_i$ and $\mathbf{x}_j$, i.e., $\langle \nabla_\theta L(\theta, \mathbf{x}_i), \nabla_\theta L(\theta, \mathbf{x}_j) \rangle$. Here, L denotes the used loss function and ∇_θ the derivative of a neural network w.r.t. to its parameters. In the following, we will use the gradient covariance matrix $\mathbf{C}_k$, noting that the eNTK is just the unnormalized gradient covariance matrix [68]. Given sample indices i and j, the gradient covariance matrix is defined as

$$\mathbf{C}_k[i,j] = \frac{\langle \nabla_\theta L(\theta, \mathbf{x}_i), \nabla_\theta L(\theta, \mathbf{x}_j) \rangle}{\|\nabla_\theta L(\theta, \mathbf{x}_i)\| \|\nabla_\theta L(\theta, \mathbf{x}_j)\|} \ . \tag{9}$$

In practice, it is impossible to compute this matrix over the complete state space $\mathcal{X}$ of a deep RL environment. Thus, it is commonly approximated with k samples. From a generalization perspective, $\mathbf{C}_k$ gives insights into whether updates between a pair of inputs $\mathbf{x}_i$ and $\mathbf{x}_j$ *generalize*. This is the case when the dot product of their gradients is positive. When it is negative, it means that updates between samples do not generalize, but instead *interfere* [66]. From an optimization perspective, a pronounced block structure of the gradient covariance matrix indicates a sharp and unstable loss landscape. Additionally, when $\mathbf{C}_k$ is low-rank, i.e., when most values are positive or negative values of similar magnitude, then

the network has learned a degenerate function. This means that updates on single samples generalize to the whole input space [68], making it difficult to distinguish between individual samples. The leftmost plot in Figure 1 provides an example of the gradient covariance matrix for highly collinear gradients.
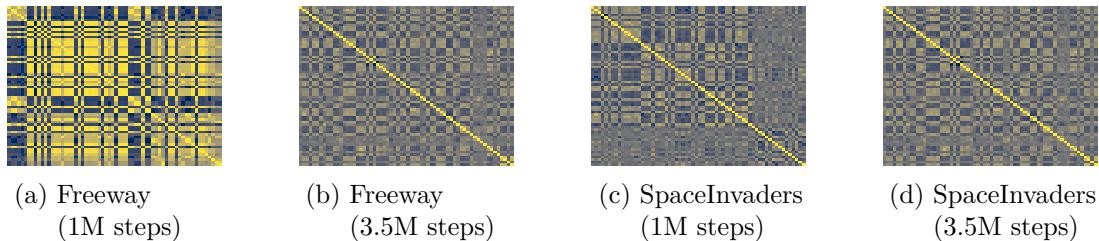

| (a) Freeway | (b) Freeway | (c) SpaceInvaders | (d) SpaceInvaders |
| (1M steps) | (3.5M steps) | (1M steps) | (3.5M steps) |

Figure 1: **Gradient covariance structure at different time steps on Atari**. *(a)* For the Atari game Freeway, the gradient covariance matrix displays a pronounced structure at one million steps. *(b)* Later in the training, the structure becomes less noticeable at 3.5M steps. *(c)* and *(d)* show the gradient covariance matrices for the game SpaceInvaders at the same time steps. Here, the structure is less pronounced. We can observe that the structure of the gradient covariances and their evolution depends on the particular game/environment.

2.5 Common Benchmarks in Deep Reinforcement Learning and Plasticity Loss

For this section, we abstractly use the term plasticity loss for a loss in a network's ability to learn and refer the reader to Section 4.1 for a formal definition. Factors commonly leading to a loss of learning ability can either occur naturally as part of a learning task or be induced artificially, enabling us to establish two categories of benchmarks for plasticity loss: The first category consists of RL environments, whereas the second consists of stationary datasets from supervised learning with (artificially) added non-stationarity. We start by reviewing the commonly used RL environments before discussing the artificially generated non-stationary datasets.

The most widely-used RL benchmarks to evaluate plasticity loss are the Atari suite [7] and the DeepMind Control Suite [99]. Both have in common that they are very well-established and provide a wide range of environments with different characteristics and difficulties. Atari differs from DeepMind Control in that its action space is discrete, whereas DeepMind Control uses a continuous action space. Additionally, DeepMind Control allows for training from image observations and vector states, whereas Atari only entails training from images[1]. Due to the diversity of both benchmarks, they include environments where either plasticity loss or the associated pathologies occur strongly. For Atari, plasticity is lost for instance during training on Phoenix [83] and Space invaders, whereas Demon Attack suffers from inactive neurons [97]. For DeepMind Control, all tasks associated with

---

1. The Atari suite allows training on 1024 dimensional RAM states [7], but this is not a commonly used benchmark.

the DOG environment pose a significant challenge to current algorithms due to quickly exploding gradient norms [80].

Regarding other benchmarks, Atari-100k [52] is a subset of the full Atari suite consisting of 26 games, where the goal is to achieve the maximum possible reward within 100,000 steps. For model-free algorithms, this entails training with many updates per environment step, often exacerbating plasticity loss [25, 82]. For continuous control, the MuJoCo environments [100] are still used in some papers but have mostly been superseded by DeepMind Control, as evidenced by the number of papers using either of them recently. MetaWorld [111] is a benchmark for continuous control in robotics, containing 50 distinct tasks. From the perspective of plasticity loss, Nauman et al. [80] show that MetaWorld exhibits different pathologies than DeepMind Control, e.g., the parameter norms and gradient norms of the agent play more of a role in determining agent performance. This makes it a useful benchmark to use alongside DeepMind Control, enabling verification of algorithms on environments with substantially different characteristics.

Utilizing the widely-used MNIST dataset as a foundation, *Permuted MNIST* is a continual learning benchmark where the pixels of the individual MNIST images are shuffled for each new task [23]. An alternative to pixel shuffling is label permutation [66], where the class labels are changed. For example, this could assign all nines the label "one" in MNIST. Label permutation differs from label randomization in that labels are changed *consistently across classes*, whereas for label randomization, the changes must not be consistent for a class. In contrast to assigning all nines the label "one" for permutation, randomization would amount to drawing a new, random label for each individual sample. Label randomization can also be applied to only a fraction of a dataset, termed *label noise* in the literature [47, 62]. These modifications can also be applied to other image datasets, such as CIFAR-10 [47] or ImageNet [23]. A specific benchmark building on ImageNet is *Continual ImageNet* [23], where the network has to solve a sequence of binary classification tasks. For each task, two labels with the corresponding samples are chosen from the 1000 labels of ImageNet. This results in the network solving a new task for each sequence step, as neither the input images nor the labels have been seen previously [23].

All benchmarks from above building on supervised learning datasets use classification tasks. In contrast, value-based deep RL uses regression with mean-squared error as loss [39, 75]. Utilizing this insight, Lyle et al. [68] define a regression benchmark using oscillating targets based on CIFAR-10 inputs. Here, each sample gets assigned a random target $y_i = \sin\left(10^5 \cdot f_\psi(x_i)\right) + b$, where b is an "offset" or bias parameter and ψ the parameter of a randomly initialized network. The bias parameter b allows controlling the magnitude of the target, which is potentially associated with plasticity loss as discussed in Section 5.6.

Lastly, a particularly relevant training scenario is *warm-starting* [5, 10, 62], which refers to pre-training a network on one task before fine-tuning it on another task. This type of two-stage training is, for example, ubiquitous when using large foundation models. We can evaluate loss of plasticity when warm-starting by pre-training a model with one of the aforementioned non-stationarities, i.e., label noise, label shuffling, or a dataset with reduced size, followed by a second training stage, where the full and correctly labeled dataset is available. If the warm-started model shows subpar performance compared to a model trained only on all samples with correct labels, it is a strong indicator that it has lost plasticity [10, 27, 62, 68].

Table 1: **Commonly used benchmarks for plasticity loss.** RL benchmark suites are in the upper half of the table with white background. As RL training is naturally non-stationary, there is no need to add nonstationarities artificially. The lower half of the table contains plasticity loss benchmarks based on supervised learning datasets (gray background). Almost all of these use classification tasks, making their "action space" discrete. Because there are multiple ways of introducing non-stationarity into a stationary dataset, we explicitly list all of them.

Benchmark	State Space	Action Space	Non-stationarity type	Used by
MetaWorld [111]	Vector states	Continuous	RL	[80], [81], [107], [51]
MuJoCo [100]	Images, Vector States	Continuous	RL	[23], [27], [26]
Atari [7]	Images	Discrete	RL	[97], [22], [83], [4], [36], [68], [67], [27], [66], [29], [65], [56]
Atari-100k [52]	Images	Discrete	RL	[82], [25], [94], [69], [61]
DeepMind Control Suite [99]	Images, Vector States	Continuous	RL	[82], [25], [14], [69], [107], [51], [61], [15], [68], [42]
Non-stationary MNIST	Images	Discrete	Pixel shuffling [37], Label shuffling [66], Label noise [62], Small data [62]	[23], [26], [63], [66], [27], [24], [62]
Non-stationary CIFAR10	Images	Discrete	Label noise [47], Label shuffling [47], Small Data [47]	[47], [26], [68], [67], [63], [27], [66], [24], [31], [62]
Non-stationary ImageNet	Images	Discrete	Sequence of binary classification [23], Label shuffling [26], Label noise [62], Small data [62]	[23], [63], [27], [26], [24], [62]
Large magnitude regression [68]	Images	Continuous	High-frequency targets	[68], [29]

3. Related Work

In the context of deep RL, the study of plasticity loss has recently (re-)gained traction [47, 82]. Consequently, general surveys on deep RL often do not yet cover plasticity loss [3, 105], whereas newer surveys mainly cover unrelated sub-areas of deep RL, e.g., structure in MDPs [76] or credit assignment [91]. To the best of our knowledge, our survey is the first to exclusively review plasticity loss for deep RL.

The two areas most closely connected to plasticity loss are (a) continual learning, and (b) continual RL. Continual learning is concerned with learning a sequence of tasks characterized by a dynamic data distribution [104]. It occurs in many contexts, such as when fine-tuning a pre-trained model [112] or when training LLMs [106]. To enable efficient learning under distribution changes, continual learning algorithms must balance a trade-off between "*learning plasticity and memory stability*" [104]. In other words, continual learning deals with both plasticity loss and catastrophic forgetting, putting an emphasis on the latter [23]. In contrast, our survey focuses solely on plasticity loss but in a scenario where data distribution shifts occur naturally—even without changing tasks—, namely deep RL. Examples of such distribution shifts are changes in the state visitation distribution due to an updated policy or changes in an agent's target distribution due to an improved value function in TD learning (cf. Section 2.2).

In continual RL, the agent is faced not only with non-stationarity arising from changes in its own policy but also time-dependent changes to the MDP's transition and reward functions [2, 53]. From a conceptual perspective, this results in the agent facing the same stability-plasticity dilemma as a network does in supervised continual learning [104]. Our survey exclusively reviews the plasticity part dilemma. On the other hand, continual RL also comprises many RL-specific sub-areas, such as credit assignment, exploration under non-stationarity, and goal-conditioned RL [53].

4. Definitions of Plasticity Loss and Related Phenomena

In this section, we first provide and generalize definitions of plasticity loss from recent literature and then relate them to aspects of related phenomena in continual learning.

4.1 Definitions of Plasticity Loss

In the literature, there is no single accepted definition of plasticity loss. Here, we attempt to unify some existing definitions and illustrate how many definitions from the literature are special cases of our result. Intuitively, all existing definitions try to capture a model's loss of ability to fit new targets but formalize this and the underlying training and evaluation setup differently.

Our unified definition is as follows:

Definition 3 (Loss of plasticity) *Let $P_{\mathcal{X}}^{(t)}$ be a distribution over inputs $\mathcal{X}$, and $P_L^{(t)}$ a distribution over a family of real-valued loss functions L with domain $\mathcal{X}$. Let g_θ represent a neural network with parameters θ, $\mathcal{O}$ correspond to an optimization algorithm for supervised*

learning, and $\mathcal{I}$ represent an intervention *on the parameters θ. Using*

$$c^{(t)}(\theta) = \mathbb{E}_{L \sim P_L^{(t)}} \left[\mathbb{E}_{\mathbf{x} \sim P_{\mathcal{X}}^{(t)}} [L(g_\theta, \mathbf{x})] \right] \tag{10}$$

to denote the loss of the neural network at time t using parameters θ, we define the loss of plasticity as

$$\mathcal{C}(\{P_{\mathcal{X}}^{(t)}\}_{t=1}^T, \{P_L^{(t)}\}_{t=1}^T, \mathcal{O}, \mathcal{I}) = c^{(T)}(\theta^{(T)}) - c^{(T)}(\theta^{(0)}) \tag{11}$$

where

$$\theta^{(t+1)} = \mathcal{O}\left(\theta^{(t)'}, P_{\mathcal{X}}^{(t)}, P_L^{(t)}\right) \quad \text{and} \quad \theta^{(t)'} = \mathcal{I}(\theta^{(t)}, P_{\mathcal{X}}^{(t)}, P_L^{(t)}). \tag{12}$$

This definition generalizes many existing definitions in that it enables different losses at different time steps, which is, e.g., relevant for multi-task learning, and in that it allows for explicit manipulations of the parameters outside of the behavior of the optimization algorithm.[2]

Many definitions of *loss of plasticity* — sometimes referred to by a different term — in the literature are special cases of the above definition:

- Berariu et al. [10] defined the *generalization gap* as "the difference in performance between a pretrained model — e.g. one that has learned a few tasks already — versus a freshly initialized one". The notion of the already-learned tasks corresponds to different tasks given by $P_{\mathcal{X}}^{(t)}, P_L^{(t)}$ for $t = 1, \ldots, T-1$ while the performance is evaluated with respect to a final task characterized by $P_{\mathcal{X}}^{(T)}, P_L^{(T)}$. The freshly initialized model is given by $g_{\theta^{(0)}}$ with $\theta^{(0)}$ being random initial parameters.

- Lyle et al. [65] defined the *target-fitting capacity* as a measure of how well a neural network can fit a distribution of targets given by a family of labeling functions (real-valued functions mapping inputs from $\mathcal{X}$ to targets). This definition arises from Definition 3 by considering $T = 1$ and selecting $P_{\mathcal{X}}^{(t)}, P_L^{(t)}$ accordingly.[3]

- Lyle et al. [66] also define *loss of plasticity* but don't explicitly account for time-dependent distributions $P_{\mathcal{X}}^{(t)}, P_L^{(t)}$ and interventions. Their definition is thus a special case without applying any intervention and constant distributions for the input and the loss functions.

- Elsayed and Mahmood [26] provide a sample-based notion of plasticity loss corresponding to a baseline normalized version of the plasticity loss defined in Lyle et al. [66]. Their definition arises as a special case from ours by fixing the loss function (i.e., using the same loss functions for all t) while making it dependent on the optimizer and the intervention.

---

2. Clearly, interventions on the parameters, e.g., resetting parameters to revive dead neurons, could also be considered as part of the optimizer. However, making the interventions explicit and not considering them as part of the optimizer can help to explicate different mechanisms affecting the loss of plasticity.

3. There is still a slight difference between the definition in Lyle et al. [65] and our definition: our definition subtracts $c^{(T)}(\theta^{(0)})$ as a baseline.

4.2 Plasticity Loss in Other Fields and Related Phenomena

This section briefly discusses the relevance of plasticity loss in fields other than RL and its relation to other phenomena in deep learning.

Network plasticity is also a crucial property for facilitating *continual learning*, where a system learns from a sequence of data distributions, each defining a new task [78]. To succeed in continual learning, the learner must not only retain plasticity but also mitigate another well-known pathology of deep learning, namely *catastrophic forgetting* [72]. It refers to a network suddenly unable to solve a previously learned task after learning a new one. In continual learning, the system must find a balance between tackling plasticity loss and catastrophic forgetting: If the network is very plastic and immediately adapts to data from a different distribution, it is also more prone to quickly forgetting previously learned knowledge, resulting in catastrophic forgetting. The other extreme is a network with no plasticity, e.g., a network with frozen weights: It certainly cannot forget previous tasks but also exhibits no plasticity, i.e., freezing the weights corresponds to a complete loss of plasticity.

When warm-starting training by fine-tuning a pre-trained network, task shifts are arguably one reason for exacerbated plasticity loss [5, 10]. However, plasticity can also be lost quickly in RL environments [83] without an obvious task shift through a changed objective. Whether an agent in an RL environment faces a single task is a peculiar question: In value-based RL with target networks, it can be argued that with each new target network update, the agent needs to solve a new task [4]. However, completely stationary learning problems may also result in plasticity loss. For example, Lyle et al. [68] show that using large-mean targets in stationary regression is enough for networks to lose their plasticity.

Lastly, plasticity loss is a broad categorization, likely subsuming several individual phenomena and causes. As we will discuss in Section 5.5, plasticity loss entails different subcategories, such as adaptability to input distribution shifts and to target shifts [61]. Similarly, there is a *generalizability* component to plasticity loss. It occurs, for example, when a network pre-trained under non-stationarity has sub-par test performance when fine-tuned, despite comparable train performance to a network not pre-trained under non-stationarity. What is commonly referred to as plasticity loss and used as the basis for the definitions in Section 4.1, however, is *trainability*: It means that a network is unable to update its parameters, even given a high loss [1, 62].

5. Causes of Plasticity Loss

This section presents and categorizes possible causes of plasticity loss from the literature. Note that these causes reside on different conceptual levels: For instance, non-stationarity (Section 5.5) is a common high-level property of a learning problem that seems to occur in almost all settings where plasticity loss occurs. In contrast, the curvature of a neural network's optimization landscape discussed in Section 5.4 is a very specific network property. Furthermore, we review saturated neurons in Section 5.1, collapse of a network's effective rank in Section 5.2, gradient issues of networks that have lost plasticity in Section 5.3, the regression loss in Section 5.6, and parameter norms in Section 5.7. Training with high replay ratios, which refers to doing many gradient updates per environment step, is discussed in Section 5.8, followed by early overfitting (Section 5.9). Having finished the exposition of
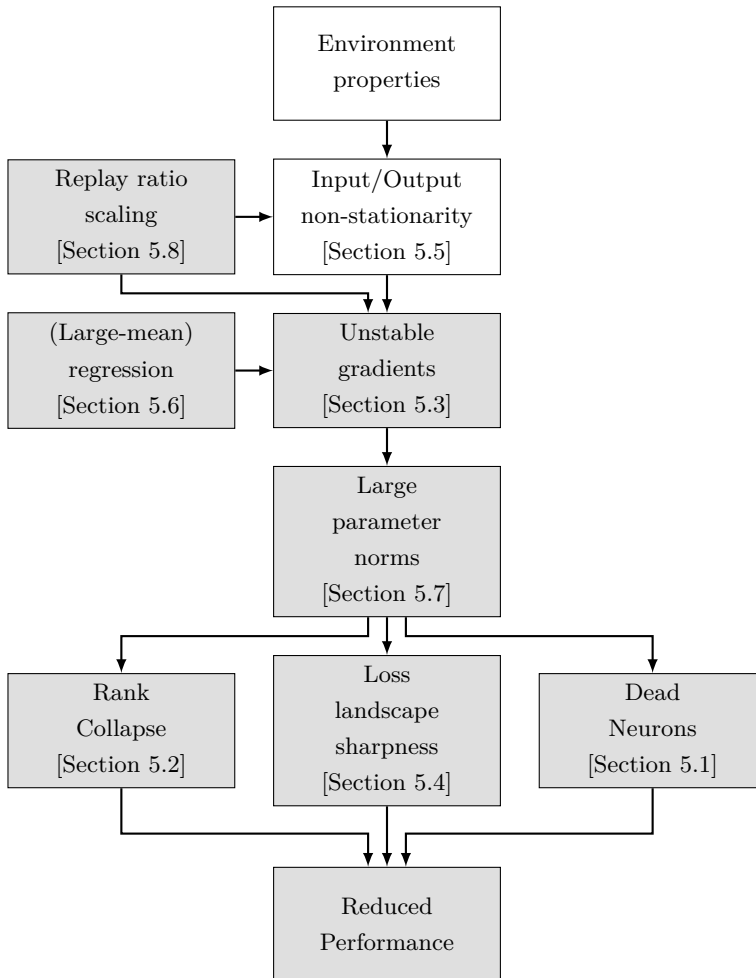
Figure 2: **Possible connections between factors and causes of plasticity loss in value-based RL**. Large-mean regression targets combined with non-stationarity of deep RL training cause large and unstable gradients, leading to an increase in parameter norms. Large parameter norms are known to increase loss sharpness and cause other pathologies, together leading to reduced agent performance.

potential causes of plasticity loss, we examine relationships between them in Section 5.10. Figure 2 relates different network pathologies and possible causes of plasticity loss.

5.1 Reduced Capacity due to Saturated Units

Saturated [15, 68] or dormant [97] units are one of the most prominent pathologies associated with reduced agent performance and plasticity loss. They are an obvious and objectively measurable sign indicating that the network cannot utilize its full capacity. Therefore, it is easy to relate them to reduced network expressivity and slow learning [97]. However, it is unclear whether dormant neurons are the main cause of plasticity loss or are just

a pathology associated with networks that have lost their plasticity. For example, Sokar et al. [97] discuss target non-stationarity as contributing to an increase in dormant neurons throughout training. Other aspects of modern deep RL algorithms might also exacerbate the phenomenon, such as training with high replay ratios [25, 94].

How can units with reduced capacity be formally defined? The literature provides a plethora of options to do this, which we group into two categories: *Saturated units* for which a shift in the pre-activation distribution reduces the capacity of the neuron to produce meaningfully different outputs given inputs from its input distribution. For example, this could be a ReLU neuron where all inputs are positive or negative, rendering it inactive ("dead") [70] or linear [68], respectively. *Dormant units* [97] are instead characterized by low post-nonlinearity activations. When considering a tanh unit, one can easily see how these categories differ: For large pre-activations, the unit's output will be close to one for all inputs. Importantly, the output will be close to one (i.e., show small numerical differences), even considering significant differences in the pre-activation. On the other hand, such a saturated tanh unit is clearly not dormant because its post-nonlinearity activation is high.

Saturated Neurons have first been discussed in Bjorck et al. [15] in the context of pixel-based continuous control. The authors took a closer look at runs of the then-state-of-the-art agent DrQ-v2 [110] and observed that most of them exhibited saturated tanh policies, with runs failing to learn and not being able to move out of this regime[4]. This results in actions at the boundaries of the $[-1, 1]$ interval from which actions are usually selected in continuous control combined with vanishing gradients, as $\forall \mathbf{x} \colon |\tanh(g_\theta(\mathbf{x}))| \approx 1 \implies \frac{\partial}{\partial \theta} \tanh(g_\theta(\mathbf{x})) = [1 - \tanh^2(g_\theta(\mathbf{x}))] \frac{\partial}{\partial \theta} g_\theta(\mathbf{x}) \approx 0$. Interestingly, their proposed solution to normalize the features of the penultimate layer increases performance when applied not only to the actor but also to the critic [15], highlighting the fact that bounded activations may be just as important to prevent critic divergence [12].

More recently, Lyle et al. [68] partition non-stationary learning problems into an *erasing or unlearning phase* and a *disentanglement phase*, finding that the first causes a form of saturation in ReLU units. These *linearized units* are characterized by their pre-activation distribution having only positive support. To be more precise, the unlearning phase after a task shift causes a distribution shift in the neuron's pre-activation distribution through gradients that either increase or decrease the preactivation values for all training samples. If all pre-activations for a neuron are now positive, the unit becomes *linearized*, removing its nonlinear component. If a neuron's pre-activations are negative for the training dataset, it moves into the dead neuron regime. Both of the aforementioned pathologies effectively reduce the expressive capacity of the network. As a remedy, the authors propose to apply LayerNorm [6] before a unit's nonlinearity [68].

Dormant Neurons have been introduced by Sokar et al. [97] as a measure for the reduced expressivity of a neural network. In experiments, they have shown that dormant neurons are associated with performance plateaus and reduced performance of DQN [75] agents trained on different Atari games. To determine the level of dormancy, one has to first calculate

---

4. DrQ-v2 builds on top of TD3 [33], which is an agent based on deterministic policy gradients that uses the tanh function to clip actions in $[-1, 1]$.

normalized activation scores s_i^l for each neuron i in all non-final layers l [97]:

$$s_i^l = \frac{\mathbb{E}_{\mathbf{x} \in \mathcal{D}}\left[|h_i^l(\mathbf{x})|\right]}{\frac{1}{H^l} \sum_{k \in [H^l]} \mathbb{E}_{\mathbf{x} \in \mathcal{D}}\left[|h_k^l(\mathbf{x})|\right]} \ . \tag{13}$$

Here $\mathbf{x} \in \mathcal{D}$ are samples drawn from an input distribution, e.g., the replay buffer in off-policy deep RL, $h_i^l(\mathbf{x})$ denotes the post-nonlinearity activation of a neuron in layer l, and H^l the number of neurons in layer l.

Neuron Dormancy

If the score in Equation (13) is below a threshold τ, i.e., $s_i^l \leq \tau$, then neuron i in layer l is τ-*dormant*. Denoting H_τ^l as the number of dormant neurons per layer, and N^l as the total number of neurons per layer, the *dormancy ratio* is the fraction H_τ^l/N^l of all layers except the final layer [97, 107]:

$$\beta_\tau = \sum_{l \in \theta} H_\tau^l / \sum_{l \in \theta} N^l \tag{14}$$

An agent exhibits the *dormant neuron phenomenon* if its fraction of dormant neurons increases over the course of the training.

The above definition is certainly not the only sensible way of defining a measure for neurons with reduced activity, but it is currently widely accepted within the literature [69, 84, 85, 97, 107] due to its simplicity and intuitive understanding. Dohare et al. [23] define a more complex measure of neuron utility based on a product between the magnitudes of a unit's summed weights and its activations. A more straightforward option for ReLU networks is to simply count the number of zero activations [1, 26].

To summarize: While there are different options for defining inactive neurons [23, 26, 97], all of the works cited above agree that they are a symptom of reduced expressivity caused by some form of non-stationarity [1, 69, 97]. Where they differ is in the proposed solution to address inactive units: Sections 6.1 and 6.2 discuss a plethora of reset strategies as possible remedies [23, 82, 97, 107], Section 6.5 considers activation functions for non-stationary problems such as CReLU [1], and Section 6.3 examines parameter regularization [63].

5.2 Effective Rank Collapse

Multiple works observe a correlation between an agent's performance degradation and its representation becoming low-rank. This phenomenon is dubbed "rank collapse" and has been observed both in online [42, 56, 65] and offline [38, 56] RL. Kumar et al. [56] establish a connection between the effective rank of an agent's representation and its ability to learn: A decrease in the representation's rank leads to increased TD error. In theoretical and empirical analysis, Kumar et al. [56] show that a drop in rank comes by the largest singular values of the representation outgrowing the smaller ones, most likely caused by bootstrapping in value-based deep RL. This effect may be exacerbated in sparse-reward environments such as Montezuma's revenge on Atari [66]. Gülçehre et al. [38] presents a thorough empirical study and find that the association between effective rank and agent performance is not as straightforward as previously assumed in offline RL. In particular,

it depends on potentially confounding hyperparameter and architecture choices, such as the activation function and the learning rate. However, they show that the collapse of the effective rank to a very small value is reliable and allows for identifying underfitting agents with suboptimal performance at the end of training.

The phenomenon of rank collapse is tightly intertwined with other phenomena pertaining to loss of plasticity. In offline RL, there is a strong correlation between the effective rank and the number of dead units in the agent's network [38]. Similarly, resetting dead or dormant neurons increases feature rank at the end of online RL training [97]. As of now, the exact causal relationship between dead neurons and rank collapse is unclear.

5.3 First-order Optimization Effects

Deep neural networks are most commonly trained using stochastic gradient descent (SGD); looking at a neural network's gradients is, therefore, a plausible direction to look for causes of plasticity loss. *Vanishing gradients* [44] are a well-known issue in training recurrent neural networks and may also play a role in the loss of plasticity. In particular, a collapse in the L0 and L1 gradient norms[5] despite high loss values is an indication that the agent isn't able to adapt despite its network being of sufficient capacity to do so [1]. A collapse in the L0 norms indicates increased gradient sparsity, which may contribute to more sparse ReLU activations and dead neurons [1]. A more nuanced notion of sparsity is *gradient dormancy*, which is closely related to neuron dormancy discussed in Section 5.1, but using the gradient L2 norms instead of neuron activations in its calculations [51]. Ji et al. [51] show that gradient dormancy is an issue faced by proprioceptive control agents in sparse-reward tasks, indicating a connection between sparse feedback, learning ability, and representation quality of an agent [64].

On the other end of the spectrum, *exploding gradients* are a clear sign of divergence and have been shown to occur when trying to scale deep RL networks [14] or in high-complexity environments, such as DM control's DOG [80]. However, it is worth emphasizing that the occurrence of large gradient norms is highly environment-dependent: While DOG suffers severely, the phenomenon is less pronounced on MetaWorld and even less of an issue on non-DOG DM Control [80]. Both vanishing and exploding gradients are easy to detect, although the latter usually has more severe performance implications than the former.

A more subtle gradient-related optimization issue is gradient collinearity [66], which refers to the structure of the gradient covariance matrix or empirical neural tangent kernel (eNTK) [68], measuring how well gradients for one sample generalize to other samples. If this matrix has a diagonal structure, updates don't generalize, leading to overfitting. If all entries have the same value, then gradients from one sample generalize to all other samples, indicating that the network has learned a degenerate function [68]. For value-based deep RL, the eNTK often has a very clear structure, as shown in Figure 1. Many methods mitigating plasticity loss weaken this structure and reduce the correlation between gradients, such as LayerNorm, weight clipping, and pruning [27, 66, 68, 85]. This hints at highly correlated gradients being a sign of an ill-conditioned optimization landscape, potentially causing plasticity loss [66].

---

5. Abbas et al. [1] note that the L2 gradient norm can be misleading due to the potentially disproportional weight of a few outliers.

5.4 Second-order Optimization Effects

It is well-known from supervised learning that flat minima generalize better [31, 45]. Connecting to this insight, there is a growing body of work linking plasticity loss with the sharpness of a network's optimization landscape: Networks that have lost plasticity usually also display high curvature [63, 66]. Lyle et al. [66] find that increased curvature as measured by the largest eigenvalue of a network's Hessian makes optimization more difficult and leads to plasticity loss. In a similar vein, Lewandowski et al. [63] argue that a collapse of the Hessian's effective rank [56] (cf. Definition 1) is causing plasticity loss. To measure curvature, they find that the empirical Fisher information matrix outperforms other approximations, such as the Gauss-Newton approximation, in terms of accuracy [63]. If a sharp optimization landscape were to cause plasticity loss, then methods explicitly reducing sharpness, such as the SAM optimizer [31], should also mitigate it. Lee et al. [61] evaluate SAM in an Atari-100k agent and find it very effective at reducing sharpness as measured by the Hessian's largest eigenvalue. However, their ablation studies highlight that resets [82] (cf. Section 6.1) still outperform SAM in terms of cumulative reward when applied in isolation. The performance gap between resets and SAM occurs despite significantly higher curvature when applying resets, indicating that sharpness cannot be the sole cause behind plasticity loss. Lee et al. [61] attributes this performance gap to smooth minima only reducing sensitivity to changes in the input distribution, whereas complementary methods must tackle the orthogonal issue of changes in the target distribution.

5.5 Non-stationarity

Non-stationarity is simultaneously the most likely culprit for causing plasticity loss and one of the most elusive [23, 47, 61, 62, 65]. What type of non-stationarity causes networks to lose plasticity? Which capabilities of a network are affected? How can non-stationarity even be quantified? Intuitively, non-stationarity makes sense as a driving mechanism of plasticity loss. Practically, verifying whether it is the sole underlying cause or to what extent non-stationarity causes networks to lose their ability to learn is difficult. In the following, we give an overview of different aspects of non-stationarity, which are partially overlapping.

Input non-stationarity is defined through changes in the data distribution $P(\mathbf{x})$ [61]. In deep RL, this usually occurs due to an improving policy that generates data from a slightly different distribution with each update. Elsayed and Mahmood [26] use *input-permuted* MNIST to evaluate different methods concerning plasticity loss, where the network has to solve a sequence of classification tasks with all the pixels of MNIST images being shuffled new for each task. The idea behind input-permutation as a benchmark for plasticity is that for a network to be successful, it must re-learn its representation from scratch for each new task. In contrast, the network should be able to re-use its learned features and only have to update its head in case the labels were shuffled instead. Therefore, input permutation can be a better benchmark for plasticity than label permutation. This argument supports the hypothesis that input non-stationarity may cause plasticity loss. Other works simulate input distribution shifts by training networks on progressively expanding subsets of data, commonly based on CIFAR-10 or MINST classification [47, 61, 62, 68]. Depending on the size of the initial subset, this type of non-stationarity can have dramatic consequences:

While the network is often able to reach similar levels of training accuracy, *test accuracy* often suffers massively for smaller initial subset ratios [47, 62], even when later training on the full dataset (warm-starting). This can be seen as a form of overfitting on the first task that has a residual effect on the second task. Despite further improvements on the train dataset in the second stage, the generalization performance stagnates. An early hypothesis for explaining this phenomenon is that the network initially overfits to the smaller subsets, learning suboptimal features that are insufficient for high-performance classification on the full dataset [47]. Lee et al. [62] decompose plasticity into *trainability* and *generalizability*, indicating that current methods [1, 97] focus on the former, neglecting the latter. Instead, generalizability can be somewhat maintained by common regularization techniques such as data augmentation or weight decay in the warm-starting scenario described above. These findings (a) support the existence of the generalization gap from Section 4.1, and (b) they indicate that enhancing trainability without addressing generalizability leads to overfitting.

Target non-stationarity refers to changes in a learning problem's labels over the course of the training, that is, the distribution $P(y|\mathbf{x})$ changes [61]. In deep RL, this typically occurs due to bootstrapping: Assuming the use of target networks, each update of the target network changes the optimization problem, such that, effectively, an RL algorithm solves a sequence of optimization problems [4]. There is mounting evidence in the literature suggesting that target non-stationarity is a main driver of plasticity loss, but its exact mechanism is still unclear. Igl et al. [47] hypothesize that non-stationarity leads to the network learning suboptimal features, which are then reused and cause reduced performance over time. Similarly, Kumar et al. [56] have found that bootstrapping targets in deep RL produce low-rank representations associated with performance collapse. Bootstrapping may even cause early performance collapses that are hard to recover from when it leads to large fluctuations early in training [69]. Another study has determined whether input or target non-stationarity is causing plasticity loss by performing experiments with offline and online RL agents. They find that plasticity loss, measured by the fraction of dormant neurons, still exists in offline RL. The authors conclude that target non-stationarity is the key factor [97]. This has been verified in toy experiments, where a network has to memorize labels on a sequence of MNIST tasks or regress on targets with increasing magnitude. Both types of non-stationarity lead to growing parameter norms, one of the pathologies commonly associated with plasticity loss and suspected of inhibiting learning [68]. Interestingly, Elsayed and Mahmood [26] argue that maintaining performance in the presence of target distribution shifts is more of a *catastrophic forgetting* problem. This is because the main challenge with moving targets is the agent maintaining its representation in the face of distribution shifts. In theory, the agent should be able to cope with changing labels simply by adapting its last layer [26], whereas input distribution shifts require the full network's plasticity because the representation has to be relearned with each new task.

In summary, the evidence that non-stationarity plays a role in plasticity loss seems overwhelming. While research into the mechanisms as to how exactly non-stationarity causes plasticity loss is still in rather early stages, some recent works have started to provide plausible hypotheses for the phenomenon [67, 68]. Similarly, splitting up the hand-wavy argument that "non-stationarity causes plasticity loss" into more fine-grained hypotheses pertaining to individual aspects such as input and label plasticity [61] will help to advance

our understanding. As of now, it is still unclear whether the currently known facets of plasticity loss capture all relevant angles or whether more is to be discovered, e.g., trainability and generalizability [62]. From a deep RL perspective, developing toy scenarios for analysis that more closely mimic the peculiarities of common RL benchmarks will also be useful. For example, most of the works listed above use classification on MNIST or CIFAR to verify their initial hypotheses, despite most deep RL approaches using regression losses, which can have different characteristics [29, 68].

5.6 Regression Loss

Classification tasks have been observed to be easier for deep neural networks than regression ever since the AlexNet breakthrough in image classification [29]. Because value-based deep RL methods use a regression loss, recent work has hypothesized that regressing on non-stationary targets might be one of the leading causes of deep RL's optimization issues [29, 68]. For example, the two-hot trick [93] has been successfully applied to train value networks and subsequently been linked to plasticity loss, albeit at a performance cost [66]. Farebrother et al. [29] find that reformulating regression as classification using a method called HL-Gauss [49] improves RL agents in many ways such as representational capacity, robustness to noise and uncertainty, and sample efficiency. However, they do not provide deeper insights into the exact mechanisms behind regression optimization issues.

A recent investigation into the mechanisms driving plasticity loss hypothesizes that *regression with large-mean targets* causes networks to lose plasticity even in stationary learning problems [68]. This issue is particularly prevalent in value-based deep RL, where an agent ideally improves throughout training, resulting in temporal difference targets with increasing magnitude. Regressing on large-mean targets has two negative side effects: First, deep networks are prone to encoding the target offset into their weights instead of the bias. This leads to an explosion of the singular values of the corresponding dimensions in parameter space, resulting in an ill-conditioned feature matrix [68]. Second, when the network predicts the large-mean targets insufficiently well, the squaring in the MSE yields large error terms. As gradients are proportional to errors in regression tasks, these large errors blow up the parameter norms of the network [29, 68]. This growth of the parameter norms is associated with a wide range of pathologies such as poor generalization [27], loss landscape sharpness [68], and finally plasticity loss [68].

5.7 Parameter Norm Growth

Lyle et al. [68] found that parameter norm growth is a common concomitant of networks that have lost plasticity and is associated with reduced task performance. In the following, we present four possible mechanisms to explain this effect. First, Lyle et al. [68] link growing parameter norms and the sharpness of the optimization landscape: As the norms of the parameters grow, so does the maximum eigenvalue of the Hessian. This connects to the works described in Section 5.4, hypothesizing that curvature may explain plasticity loss. The same authors also hypothesize that large parameter norms may cause nonlinearities within the network, such as activation functions or softmax heads saturating. The effects of saturated units are described in detail in Section 5.1, but among them are gradient propagation issues and a loss in effective network capacity, both of which are associated

with plasticity loss. Third, it has been found that growing parameter norms may lead to gradients with sparse and/or collinear gradient covariance matrices. As a result, updates may over-generalize or under-generalize in the sample space. In an extreme case, an over-generalizing network may learn a degenerate function assigning similar outputs to all inputs. On the other hand, an under-generalizing network can only memorize task labels [68]. Both states are linked to plasticity loss. Lastly, a recent study finds that large parameter norms affect the effective learning rate of a network. In particular, as the parameter norms of a network grow, so does the norm of its gradient, leading to instability and potential plasticity loss during training [67]. The implicit effect of parameter norms on the learning rate can be mitigated with a technique called Normalize-and-Project, which we discuss in Section 6.9.

5.8 High Replay Ratio Training

The *replay ratio* (RR), sometimes also called the update-to-data (UTD) ratio, describes the number of gradient updates per environment step [19, 82] for off-policy deep RL agents. For example, the original DQN agent uses $RR = 0.25$, corresponding to one gradient step every four environment steps [75], whereas SAC uses $RR = 1$ [39]. Many algorithms do not use higher RRs to trade off sample efficiency against compute efficiency because applying more gradient updates leads to performance degradation and degenerate policies [25, 82]. This has been attributed to overfitting on early samples [82] or, more recently, early plasticity loss [25]. Ma et al. [69] hypothesize that higher RRs exacerbate initial target non-stationarity, which in turn causes agents to lose plasticity early in training. A common intervention to alleviate adverse effects from high RR training in off-policy deep RL is the application of resets, which have been shown to work well on a wide range of benchmarks [25, 80, 81, 82, 94].

Is high replay ratio training the main cause of plasticity loss? In our view, this is unlikely: Plasticity loss also occurs in scenarios without high RR training, for example, when using a standard Double DQN agent on the Atari games Phoenix and Space Invaders [83]. It seems that high RRs *amplify* plasticity loss instead of directly causing it. This argument is supported by Nauman et al. [80], who note that high RRs induce different training dynamics than low RRs. A prominent example is DeepMind Control DOG, in which SAC agents with high RRs suffer from exploding gradients [80].

5.9 Early Overfitting

When training networks under non-stationarity, some early works have hypothesized that residual effects of overfitting to early training data might hinder late training progress. The earliest work describing this phenomenon attributes it to the network trying to re-use suboptimal features acquired early during training [47]. Their results on toy datasets have been confirmed in deep RL, named the "primacy bias" [82]. The primacy bias refers to a psychological phenomenon in human learning, where early experiences can have long-lasting effects on later tasks. In the context of deep RL, it refers to agents overfitting to early interactions and being unable to update their networks in the face of new data.

While these early findings regarding plasticity loss have been compelling, more recent work has moved away from the hypothesis of early overfitting towards mechanistic and

measurable explanations such as dead neurons, parameter norm growth, or feature rank collapse.

5.10 Discussion of Causes

When looking at the causes mentioned in the previous sections, it bears repeating that they are on different conceptual levels: Non-stationarity is broad and hard to quantify, whereas the number of dead neurons is a specific, measurable property of a neural network at a given time step. As of now, the research is still inconclusive about (a) how exactly the individual mechanisms causing plasticity loss work, and (b) how they are related. Additionally, it might well be possible that unknown confounding factors exist that might provide a more abstract understanding of plasticity loss.

Figure 2 schematically relates the current understanding of plasticity loss in value-based deep RL agents. It seems clear that non-stationarity, both for inputs and targets, is a driving mechanism behind networks losing their ability to learn [61, 62]. High RR training amplifies non-stationarity, exacerbating the issues stemming from it. Recently, the issues in optimizing value-based deep RL have also been tied to the usage of regression losses, which are both less amenable to the training of deep networks in general [29] and are prone to lead to large parameter norms [68]. The latter factor is likely caused by the fact that in regression, gradients are proportional to errors, causing instability for growing and/or non-stationary regression targets [29, 68]. Growing parameter norms and unstable gradients may cause numerous other pathologies commonly associated with plasticity loss, such as dead neurons or a sharp optimization landscape [68, 97]. Together, these issues lead to reduced performance and the network's failure to adapt to new targets.

While Figure 2 tries to present links between possible causes of plasticity loss, there is, as of now, no complete theory of the phenomenon available. Instead, current research notes different optimization issues and that amalgamating these factors likely causes plasticity loss. Whether these can be merged into a unified high-level understanding of the phenomenon is unclear.

6. Mitigating Loss of Plasticity

In this section, we present an overview of approaches developed to mitigate plasticity loss. Approaches based on resetting the weights of neural networks are discussed in Sections 6.1 and 6.2, followed by approaches regularizing a neural network's weights in Section 6.3 and a neural network's feature representation rank 6.4. Approaches building on the choice of a neural network's activation functions are presented in Section 6.5 and approaches leveraging beneficial properties of the categorical loss in Section 6.6. Furthermore, distillation-based approaches, other methods, and combinations of the presented approaches are discussed in Sections 6.7, 6.8, and 6.9, respectively. We conclude this section with a discussion in Section 6.10.

6.1 Non-targeted Weight Resets

Non-targeted weight resets are a simple method for tackling plasticity loss and have initially been used to mitigate early overfitting [82]. They are considered in two different flavors:

(a) *Hard resets*, where network layers are fully reset, and (b) *soft resets*, where new network weights are generated from a linear combination of the current weights and freshly initialized ones.

Hard Resets build on the observation that plasticity loss has empirically been shown to mainly manifest in the last layers of a network [10, 25, 82]—although it may affect all layers of the network to some extent. A simple sensible strategy for mitigating plasticity loss is, therefore, a periodic, full reset of the last few layers of the agent, i.e., the weights of the last few layers are replaced by new draws from the initial weight distribution. For small agents, e.g., the ones typically used for non-pixel continuous control tasks, this amounts to resetting the complete network [25, 81, 82]. In contrast, in pixel-based control environments such as Atari, the convolutional encoder is typically not reset to retain the knowledge encoded in the agent's representation [25, 82, 94].

Soft Resets [5], also known as Shrink and Perturb (S & P), have been introduced to mitigate the so-called "*generalization gap*", which is the difference in performance observed when training a freshly initialized model compared to one fine-tuning a pretrained one [10]. S & P uses a linear combination of the current weights θ_{old} and random parameters ψ from the initial weight distribution to perform the reset [25][6]:

$$\theta_{\mathrm{new}} = \alpha\theta_{\mathrm{old}} + (1 - \alpha)\psi, \; \psi \sim \text{initializer}. \tag{15}$$

For well-tuned hyperparameters α, S & P is able to restore the network's plasticity while retaining the (relevant) knowledge stored in the network. In the context of deep RL, the SR-SPR [25] agent uses soft resets for the convolutional encoder combined with hard resets for the last layers to increase the number of gradient steps per environment step on the Atari 100k benchmark [52]. Using the same combination of hard and soft resets as SR-SPR, BBF [94] incorporates a number of other improvements, such as deeper networks and discount annealing, to set the current state-of-the-art on Atari 100k.

Comparing hard and soft resets. Looking at the advantages and disadvantages of each reset type, it stands out that hard resets *only* work for off-policy algorithms with a replay buffer. Without the buffer, a reset would erase the agent's knowledge. The experience stored in the buffer acts as a "memory", quickly allowing the agent to recover lost knowledge [25, 82]. The application of hard resets is, therefore, confined to off-policy deep RL algorithms, whereas well-tuned soft resets are also applicable to on-policy algorithms. S & P has been shown to improve a variety of metrics associated with the loss of plasticity: It decreases the number of dead neurons, prevents vanishing gradients, and prevents weight norms from exploding [26]. However, it may be possible that resets have other positive effects on deep RL training orthogonal to mitigating loss of plasticity. For example, Xu et al. [107] hypothesize that S & P may improve exploration, presumably via inducing more rapid policy change [92].

---

6. In the original work by Ash and Adams [5], the reset is defined as $\theta_{\mathrm{new}} = \lambda\theta_{\mathrm{old}} + \gamma\psi$. We choose to use the definition that is more common in deep RL.

6.2 Targeted Weight Resets

Instead of arbitrarily resetting the network's weights or parts of it, algorithms with *targeted weight resets* track some measure of utility for each neuron/layer and perform resets based on it. This allows resetting only the parts of a network that are likely affected by plasticity loss at the cost of additional computational [23, 26, 97] and memory demands [23]. A special case of this class of approaches is plasticity injection [83], which does not track any measure of utility but resets the last layers of a network in a specific way ensuring not to change its outputs.

Continual Backprop (CBP) is a reset algorithm building on top of a heuristic measure of neuron utility [23]. After each gradient step, this measure is updated for each neuron and used to reset the $x\%$ least useful neurons in each layer. As a reset strategy, CBP replaces the ingoing weights of a neuron with fresh weights sampled from the initialization distribution and sets the outgoing weights to zero. CBP also resets moment estimates of the employed Adam optimizer for the selected neurons. Lastly, the algorithm tracks a count for each neuron, measuring the number of update steps since the last reset, preventing the same neurons from being reset over and over during training. The authors show promising results on toy problems such as input-permuted MNIST or in proprioceptive RL environments. However, the necessity to track multiple metrics for each neuron and perform updates and resets at every step makes CBP expensive both in terms of memory and computation.

ReDo has been developed concurrently with CBP and uses a more lightweight notion of neuron utility that is easier to track. Instead of updating a utility measure at every gradient step, ReDo assesses every k time steps whether the per-layer normalized activations of a neuron are below a threshold τ. If they are, it resets all of these *dormant neurons* with the same strategy as CBP, namely resampling ingoing weights from the initialization distribution and setting outgoing weights to zero. On Atari, ReDo has improved the performance of DQN [75] and DrQ [109] agents substantially, particularly in games like SpaceInvaders or Seaquest, where plasticity loss is known to occur. For Soft Actor-Critic (SAC) [39] agents, performance improvements are less pronounced, likely due to proprioceptive continuous control agents exhibiting different dynamics in terms of dormant neurons than pixel-based Atari games [51].

UPGD is a noisy SGD variant focusing on both plasticity loss and catastrophic forgetting in continual learning [26]. It consists of two components: First, it adds Gaussian noise to the gradients. Second, it scales the learning rate by a measure of neuron utility U. Let θ denote the weights of a neural network. Formally, a UPGD step can be written as:

$$\theta_{l,i,j} \leftarrow \theta_{l,i,j} - \alpha \left(1 - \bar{U}_{l,i,j}\right) \left(\frac{\partial L}{\partial \theta_{l,i,j}} + \xi\right), \tag{16}$$

where $\xi \sim \mathcal{N}(0,1)$ and $\bar{U}_{l,i,j} \in [0,1]$ is the exponential moving average of the utility of the scalar parameter i,j in layer l. The term $(1 - \bar{U}_{l,i,j})$ leads to important weights not being changed due to their utility being close to 1, whereas unimportant weights will be both updated through SGD and perturbed via Gaussian noise. Intuitively, this can be seen as a targeted reset weighted by a continuous measure of parameter utility. The utility is intended to approximate a causal measure of weight utility based on an intervention,

given in Equation (17) below: *"How would the loss change if parameter $\theta_{l,i,j}$ would be set to zero?"*. As this would be expensive to compute exactly for deep networks, the authors instead estimate it with a Taylor expansion around zero for the current parameters θ [26], avoiding the need for an additional forward pass. Equation (18) states this approximate utility:

$$U_{l,i,j}(\mathbf{x}) = L\left(\theta_{\neg[l,i,j]}, \mathbf{x}\right) - L(\theta, \mathbf{x}) \tag{17}$$

$$\approx L(\theta, \mathbf{x}) + \frac{\partial L(\theta, \mathbf{x})}{\partial \theta_{l,i,j}}\left(0 - \theta_{l,i,j}\right) + \frac{1}{2}\frac{\partial^2 L}{\partial \theta_{l,ij}^2}\left(0 - \theta_{l,i,j}\right)^2 - L(\theta, \mathbf{x})$$

$$= \underbrace{-\frac{\partial L(\theta, \mathbf{x})}{\partial \theta_{l,i,j}}\theta_{l,i,j}}_{\text{first-order utility}} + \underbrace{\frac{1}{2}\frac{\partial^2 L(\theta, \mathbf{x})}{\partial \theta_{l,i,j}^2}\theta_{l,i,j}^2}_{\text{second-order utility}}, \tag{18}$$

where $\theta_{\neg[l,i,j]}$ denotes the parameters θ with parameter l, i, j set to zero. Here $\mathbf{x}$ denotes a sample, e.g., a state-action pair in RL. While in principle, the Taylor expansion could be made arbitrarily accurate, practically, even second-order expansions are expensive to compute. Under this consideration, the first-order approximation appears to show a reasonable compute vs accuracy trade-off [26]. Even though Equation (16) states the update for SGD, the UPGD algorithm can also be extended to momentum-based optimizers like Adam [26, 54].

Plasticity Injection [83] builds on the idea that plasticity loss is usually concentrated in the head of a neural network [25] and resets the last layers of an agent's neural network in the following way: At step T, it freshly initializes the last two layers of the agent's neural network such that its outputs and the number of learnable parameters stay the same. This is achieved as follows. Let θ denote the current parameters of an agent's head, θ_1' a set of freshly initialized parameters, and θ_2' a *frozen copy* of θ_1'. If we let h_θ represent the agent's head as a function parameterized by parameters θ and specify the Q-function in the following way

$$Q(\mathbf{s}) = \underbrace{h_\theta(\mathbf{s})}_{\text{frozen}} + \underbrace{h_{\theta_1'}(\mathbf{s})}_{\text{learnable}} - \underbrace{h_{\theta_2'}(\mathbf{s})}_{\text{frozen}}, \tag{19}$$

plasticity injection produces *unaffected predictions* and *preserves the number of trainable parameters* [83]. Fulfilling these two desiderata allows the injection to be a diagnostic tool that can be used to verify the existence of plasticity loss. An agent's plasticity will be restored through the freshly initialized parameters θ_1', allowing it to further improve.

6.3 Parameter Regularization

The idea of regularizing parameter norms originates from linear regression, where it is used to cope with overfitting [77]. Avoiding Plasticity loss differs from avoiding overfitting in that the goal is not to learn a simpler model but rather to preserve the general ability of the model to learn. Parameter norm regularizers developed to tackle plasticity loss build on the fact that the initial weights allow for rapid adaptation to new targets and thus aim to preserve certain properties of the initial weights via regularization. Such properties

include the rank of the learned representation, the rank of the network's Hessian matrix, or the (low) magnitude of the learned parameters. For example, low weight magnitudes are deemed to be beneficial for training, likely by inducing a smoother optimization landscape through smaller gradient norms [68].

L2 Regularization (Weight Decay) is the most prominent weight regularization method. When applied to linear regression, the resulting method is called ridge regression. From a probabilistic perspective, L2 regularization can be seen as assuming a standard Normal distribution as prior for the weights of layer l $\mathbf{W}_l$. Formally, the prior is of the form $p(\mathbf{W}_l) = \mathcal{N}(\mathbf{W}_l \mid \mathbf{0}, \mathbf{I})$. From this assumption about the prior, one can derive a penalty term using the squared L2 norm of the weights for all n layers:

$$L_{\text{L2reg}}(\theta) = L(\theta) + \lambda \sum_{l=1}^{n} \|\mathbf{W}_l - \mathbf{0}\|_2^2, \tag{20}$$

where $\mathbf{W}_l$ are layer l's weight matrices, and λ is a hyperparameter that determines the strength of the regularization. While well-tuned L2 regularization is able to keep parameters magnitudes small, in the context of RL it often interferes with training, particularly for value-based agents [68].

Spectral Normalization (SpectralNorm) is a technique for discriminator regularization in Generative Adversarial Networks (GANs) [74]. It directly controls the L2 matrix norm of layer l's weight matrix by dividing that matrix by the largest singular value $\sigma_{\max}$:

$$\mathbf{W}_l \leftarrow \frac{\mathbf{W}_l}{\|\mathbf{W}_l\|_2} = \frac{\mathbf{W}_l}{\sigma_{\max}}. \tag{21}$$

By applying SpectralNorm to all layers of the GAN discriminator, it is possible to constrain the network to be K-Lipschitz, where K is a hyperparameter to be tuned. In deep RL, it has been observed that SpectralNorm has two desirable effects for gradient-based optimization. First, it prevents exploding gradients, which is an issue when scaling RL agent networks [14, 80]. Second, SpectralNorm implicitly schedules the learning rate of the Adam optimizers, preventing performance plateaus [36]. This effect is akin to LayerNorm's implicit learning rate scheduling described in the previous paragraph [67]. Furthermore, it is more effective at mitigating overestimation bias than many techniques specifically targeted at mitigating overestimation bias, such as clipped double Q learning [80]. Nauman et al. [80] also show that SpectralNorm substantially reduces the number of dormant neurons [97] even compared to methods like ReDO that are designed to prevent dormant units [80]. Lastly, applying SpectralNorm to the penultimate layer of value-based RL agents decreases their hyperparameter sensitivity [36]. In summary, SpectralNorm positively affects a wide variety of factors commonly associated with plasticity and is thus an easy-to-use method for reducing plasticity loss.

L2 Init builds on L2 regularization by using the initial weights as regularization targets instead of the origin [24]. As the initial weights are capable of quickly fitting targets, keeping the weights closer to the initial weights instead of zero can be more desirable from the perspective of plasticity loss. Consequently, the resulting prior distribution for the

weights of layer l at step t is $p(\mathbf{W}_{l,t}) = \mathcal{N}(\mathbf{W}_{l,t} \mid \mathbf{W}_{l,0}, C\mathbf{I})$, with mean $\mathbf{W}_{l,0}$ instead of $\mathbf{0}$. This leads to the following regularized objective:

$$L_{\text{L2Init}}(\theta_t, \theta_0) = L(\theta_t) + \lambda \sum_{l=1}^{n} \|\mathbf{W}_{l,t} - \mathbf{W}_{l,0}\|_2^2. \tag{22}$$

Drawing a connection to targeted reset methods from Section 6.2, the L2 Init regularizer can be seen as a method for resetting weights that are of low importance. Compared to Continual Backprop [23] or ReDo [97], L2 Init does not explicitly calculate utilities for neurons. Instead, it implicitly determines the regularization strength for a weight based on the loss: If a gradient update for a particular weight results in a large change in loss value $L(\theta_t)$, the relative importance of the regularizing term $\|\mathbf{W}_{l,t} - \mathbf{W}_{l,0}\|_2^2$ decreases. Conversely, if changing a weight has little effect on the loss, then the regularizing term moves this particular parameter closer to its initialization value.

2-Wasserstein regularization   One problem of L2 Init is that it regularizes weights to their uninformative initial values θ_0. Lewandowski et al. [63] propose to regularize weights to their initial distribution instead of initial values. Equation (23) uses the squared 2-Wasserstein distance to enforce a small distance between the initial weight distribution p_0 and the current distribution p_t:

$$L_{\text{2-Wass}}(\theta_t, \theta_0) = L(\theta_t) + \mathcal{W}_2^2(p_t \parallel p_0), \tag{23}$$

$$\text{where} \qquad W_2^2(p_t \parallel p_0) = \sum_{l=1}^{n} \sum_{i=1}^{d} \left(\bar{w}_{l,t}^i - \bar{w}_{l,0}^i \right),$$

with $\bar{w}_{l,t}^i$ denoting the i-th largest parameter of layer l at step t. Equation (23) highlights a particular advantage of the squared 2-Wasserstein distance: The existence of a closed-form solution makes computations tractable and cheap. We can compare the 2-Wasserstein regularizer with L2 Init by writing out the L2 Init penalty in terms of individual weights:

$$R_{\text{L2Init}}(\theta_t, \theta_0) = \sum_{l=1}^{n} \sum_{i=1}^{d} \left(w_{l,t}^i - w_{l,0}^i \right).$$

As we can see, the Wasserstein regularizer is just L2 Init with *parameters sorted by their magnitude*. This subtle change allows for larger deviations of individual weights from their initial value while still keeping the current distribution over weights close to their initial distribution [63].

Weight Clipping   is another technique for preventing parameter norm growth. The idea behind weight clipping is simple: After each gradient update, ensure that weights are in a predefined range $[-b, b]$. Elsayed et al. [27] define $b = \kappa s_l$, where κ is a scaling hyper-parameter and s_l are the bounds of the uniform distribution used to initialize the weight matrix $\mathbf{W}_l$ of layer l. The big advantage of weight clipping compared to weight decay or L2 Init [24] is that it does not bias the weights towards a particular point in parameter space; instead, they can freely move within the bounds $[\kappa s_l, \kappa s_l]$. Its big disadvantage is that it only works for uniform initialization like Kaiming Uniform [27, 40].

— Parameter Regularization —

- Weight decay or **L2 regularization** mitigates overfitting in regression models by regularizing weights towards a standard Normal prior [77]:

$$R_{\mathrm{L2reg}}(\theta) = \lambda \sum_{l=1}^{n} \|\mathbf{W}_l - \mathbf{0}\|_2^2.$$

  Note that the term $\|\mathbf{W}_l - \mathbf{0}\|_2^2$ only regularizes the weight matrices; the bias terms do not contribute to overfitting.

- **SpectralNorm** enforces a Lipschitz-constraint on all weight matrices $\mathbf{W}_l$ of a network by dividing through the largest singular value $\sigma_{\max}$ of each weight matrix [74]:

$$\mathbf{W}_l \leftarrow \frac{\mathbf{W}_l}{\|\mathbf{W}_l\|_2} = \sigma_{\max}^{-1} \mathbf{W}_l .$$

  $\sigma_{\max}$ can be approximated efficiently through the power iteration algorithm.

- Dohare et al. [24] observe that the initial weights of a network possess high levels of plasticity and propose to *regularize towards the initial weights instead of zero weights* in their method **L2 Init**:

$$R_{\mathrm{L2Init}}(\theta_t, \theta_0) = \lambda \sum_{l=1}^{n} \|\mathbf{W}_l - \mathbf{W}_0\|_2^2.$$

- Lewandowski et al. [63] extend the idea of parameter regularization by *regularizing towards the initial weight distribution* via the **squared 2-Wasserstein regularizer**:

$$R_{\mathrm{2\text{-}Wass}}(\theta_t, \theta_0) = \sum_{l=1}^{n} \sum_{i=1}^{d} \left(\bar{w}_{l,t}^i - \bar{w}_{l,0}^i \right)^2.$$

  Here $\bar{w}_{l,t}^i$ denotes the i-th largest parameter of layer l at step t.

- **Weight clipping** [27] truncates the weight matrices $\mathbf{W}_l$ for each layer l with the bounds $[\kappa s_l, \kappa s_l]$, where s_l are the bounds of the uniform distribution used to initialize the layer and κ is a hyperparameter:

$$\mathbf{W}_l \leftarrow \min(\max(\mathbf{W}_l, -\kappa s_l), \kappa_s l),$$

  where the min and max operator are applied elementwise.

6.4 Feature Rank Regularization

While it is unclear whether feature rank collapse is an underlying cause of plasticity loss [66], it is a highly associated phenomenon for networks that have lost their ability to learn [23, 24]. Since the first observation that under-parameterized or low-rank representations are strongly associated with low performance in value-based deep RL [56], many algorithms have been designed to either explicitly or implicitly encourage high-rank representations.

Direct Singular Value Regularization   Kumar et al. [56] note that the effective rank from Definition 1 is non-differentiable. Let us denote $\Phi = \phi(\mathbf{X}) \in \mathbb{R}^{n \times d}$ as the matrix of

representations of dimension d for a batch of size n. To circumvent this non-differentiability issue and apply gradient-based learning, they propose to extend the loss function by a regularizer that minimizes the squared largest singular value $\sigma_{\max}^2(\Phi)$ while jointly maximizing the squared smallest singular value $\sigma_{\min}^2(\Phi)$ for a representation with parameters θ:

$$L_{\text{sing}}(\theta) = L(\theta) + \alpha \left(\sigma_{\max}^2(\Phi) - \sigma_{\min}^2(\Phi) \right). \tag{24}$$

L_{sing} is conceptually simple and applicable to any type of deep RL algorithm but suffers from instabilities. To see how potential instabilities arise, note that the regularizer is globally minimized when all singular values are exactly the same, which is achieved by a constant representation: $\Phi = \phi(\mathbf{X}) = \mathbf{0}$. This makes practical applications difficult as performance and stability are highly sensitive to the choice of the parameter α.

InFeR takes a more indirect approach towards maintaining a representation with a high effective rank by utilizing a set of k auxiliary regression tasks [65]. First, the algorithm adds k auxiliary prediction heads g_i on top of the agent's encoder ϕ_θ. Before starting the training, InFeR creates a copy of the initialization weights for both the encoder and the auxiliary task head. These weights are used to generate the regression targets for the auxiliary task using training batches from the agent's replay buffer $\mathbf{x} \sim \mathcal{D}$:

$$L_{\text{InFeR}}(\theta_t, \theta_0) = \mathcal{L}(\theta) + \alpha \mathop{\mathbb{E}}_{\mathbf{x} \sim \mathcal{D}} \left[\sum_{i=1}^{k} (g_i(\mathbf{x}; \theta_t) - \beta g_i(\mathbf{x}; \theta_0))^2 \right]. \tag{25}$$

Here β is a scaling hyperparameter for the random regression targets, and α is a coefficient for the regularization strength. Together with the number of auxiliary tasks k this introduces a number of different hyperparameters that must be tuned, which is computationally expensive. InFeR improves performance in games where plasticity loss is known to occur, such as Phoenix [83] as well as sparse-reward hard exploration games such as Montezuma's Revenge. The performance in sparse-reward settings indicates that InFeR does not just preserve effective rank but also improves exploration through its randomized regression auxiliary task.

DR3 is a method developed to prevent feature co-adaptation between successive state-action pairs in value-based deep RL [57]. This co-adaption implicitly occurs due to an implicit regularization effect of SGD updates, leading to large feature dot-products and eventually diverging Q-values. By penalizing large feature dot-products, the implicit regularization effect of SGD can be mitigated:

$$L_{\text{DR3}}(\theta) = L(\theta) + c_0 \sum_{(\mathbf{s},\mathbf{a},\mathbf{s}',\mathbf{a}')\in\mathcal{D}} \phi(\mathbf{s},\mathbf{a})^\top \phi(\mathbf{s}',\mathbf{a}'). \tag{26}$$

DR3 is not designed to explicitly maximize feature rank. However, experimental results show that it is effective at preventing rank collapse. At the same time, DR3 does not explicitly maximize rank and consequently has a lower rank than a DQN agent in games such as Breakout. Despite its lower rank, DR3 still achieves superior performance, hinting at the relationship between effective rank and agent performance being more intricate [57].

BEER adaptively regularizes the rank of a representation based on an upper bound of the cosine similarity between the representations of consecutive state-action pairs [42]. It builds on the insight that naively maximizing feature rank may lead to overly complex models and overfitting. The upper bound derived by He et al. [42] is a necessary condition for the optimal value function:

$$\cos\left(\phi(\mathbf{s},\mathbf{a}), \overline{\phi(\mathbf{s}',\mathbf{a}')}\right) \leq \left(\|\phi(\mathbf{s},\mathbf{a})\|^2 + \gamma^2\|\overline{\phi(\mathbf{s}',\mathbf{a}')}\|^2 - \frac{\|r\|^2}{\|\mathbf{w}\|^2}\right) \cdot$$
$$\frac{1}{2\gamma\|\phi(\mathbf{s},\mathbf{a})\|\|\overline{\phi(\mathbf{s}',\mathbf{a}')}\|}. \tag{27}$$

Here $\phi(\mathbf{s},\mathbf{a})$ is a state-action representation obtained from the penultimate layer of the agent, $\overline{\phi(\mathbf{s}',\mathbf{a}')} = \mathbb{E}_{s',a'}\phi(\mathbf{s}',\mathbf{a}')$ is the expected representation under the distribution for the next state-action pair, $\mathbf{w}$ are the weights for the final layer and $\|r\|^2$ is the squared reward for the transition. As minimizing the RL loss under this constraint is a non-convex optimization problem, the authors propose to use the constraint as a penalty term with weight β:

$$L_{\text{BEER}}(\theta) = L(\theta)$$
$$+ \beta \operatorname{ReLU}\left(\cos\left(\phi(\mathbf{s},\mathbf{a}), \mathbb{SG}\overline{\phi(\mathbf{s}',\mathbf{a}')}\right)\right.$$
$$\left. - \mathbb{SG}\left(\left(\|\phi(\mathbf{s},\mathbf{a})\|^2 + \gamma^2\|\overline{\phi(\mathbf{s}',\mathbf{a}')}\|^2 - \frac{\|r\|^2}{\|\mathbf{w}\|^2}\right)\frac{1}{2\gamma\|\phi(\mathbf{s},\mathbf{a})\|\|\overline{\phi(\mathbf{s}',\mathbf{a}')}\|}\right)\right). \tag{28}$$

Compared to the conceptually similar DR regularizer from Equation (26), BEER is able to adaptively adjust the rank depending on the complexity of the task. In turn, this leads to better performance and more accurate Q-values when compared to InFeR [65].

The relationship between effective rank, feature rank collapse, and plasticity loss is, as of now, still not well understood. It seems clear that rank collapse does harm a network's ability to learn [24, 38, 56], particularly for value-based deep RL agents. However, it is unclear whether maximizing effective rank is beneficial for learning. Here, He et al. [42] provide the first negative results. For offline RL, Gülçehre et al. [38] study in-depth how effective rank relates to a host of other training variables. Key findings include that rank collapse and performance are more strongly associated with ReLU networks than with tanh ones and that using high learning rates increases the chance of rank collapse. Another interesting finding of Gülçehre et al. [38] is the strong negative correlation between the number of dead units and effective rank. However, their work does not establish a causal relationship between the two quantities. To summarize: While a drop in effective rank seems to be a concomitant for networks that have lost their ability to learn, the nature and direction of a causal relationship between rank and plasticity has not been established as of now.

<div style="border: 1px solid; padding: 10px;">

Feature Rank Regularization

- Given a state-action pair $(\mathbf{s}, \mathbf{a})$, Kumar et al. [56] propose a **singular value regularizer** to directly prevent rank collapse of a representation ϕ with parameters θ:

$$R_{\text{sing}}(\theta) = \sigma_{\max}^2(\phi(\mathbf{s}, \mathbf{a})) - \sigma_{\min}^2(\phi(\mathbf{s}, \mathbf{a})).$$

  While the above penalty is computationally efficient, it is prone to representation collapse as $\theta = \mathbf{0}$ is a global minimizer of R_{sing}.

- **DR3** [57] penalizes large feature dot products between consecutive state-action pairs:

$$R_{\text{DR3}}(\theta) = \phi(\mathbf{s}, \mathbf{a})^\top \phi(\mathbf{s}', \mathbf{a}').$$

  Despite not explicitly aimed at increasing feature rank, DR3 prevents rank collapse [57] and enhances performance [58].

- **InFeR** [65] preserves the rank of a representation by regressing $i = 1, \ldots, k$ auxiliary task heads $g_i(\cdot, \theta)$ on counterparts $g_i(\cdot, \theta_0)$ with frozen initial parameters θ_0:

$$R_{\text{InFeR}}(\theta, \theta_0; \beta) = \sum_{i=1}^{k} (g_i(\mathbf{x}; \theta) - \beta g_i(\mathbf{x}; \theta_0))^2.$$

  The frozen target heads $g_i(\cdot, \theta_0)$ utilize a shared encoder ϕ_0 with frozen initialization weights.

- **BEER** [42] enforces an upper bound on the cosine similarity between successive state-action representations derived from the Bellman equation:

$$R_{\text{BEER}}(\theta) = \text{ReLU}\left(\cos\left(\phi(\mathbf{s}, \mathbf{a}), \mathbb{SG}\overline{\phi(\mathbf{s}, \mathbf{a})}\right) - \right.$$
$$\left. \mathbb{SG}\left(\left(\|\phi(\mathbf{s}, \mathbf{a})\|^2 + \gamma^2\|\overline{\phi(\mathbf{s}', \mathbf{a}')}^2\| - \frac{\|r\|^2}{\|\mathbf{W}\|^2}\right) \frac{1}{2\gamma\|\phi(\mathbf{s}, \mathbf{a})\|\|\overline{\phi(\mathbf{s}', \mathbf{a}')}\|}\right)\right),$$

  where $\mathbb{SG}$ denotes stopped gradients, $\mathbf{w}$ are the final layer weights, and $\|r\|^2$ is the squared reward for DQN-style sample backups.

</div>

6.5 Activation Functions

When looking at loss of plasticity through the perspective of dead/dormant neurons [70, 97], we can observe that some activation functions lead to more dead neurons than others. This is particularly relevant for ReLU [70], which is the most commonly used activation function in deep RL. Therefore, it is reasonable to assume that a different activation function can improve a network's plasticity. Below, we will present three activation functions used in the literature to prevent plasticity loss, with the last two being specifically designed to maintain plasticity. We will use a scalar input $x \in \mathbb{R}$ for all presented definitions as these functions are applied element-wise.

Parameterized Exponential Linear Units (PELU) are a generalization of the ELU [20] activation function with learnable parameters [35]. This allows PELU to adjust the activation slopes, yielding an ability to respond to distribution shifts akin to rational activations

described below. Using α and β to denote the learnable parameters, PELU is defined as

$$
\text{PELU}(x) = \begin{cases} \frac{\alpha}{\beta} h & x \geq 0 \\ \alpha \left(e^{\frac{h}{\beta}} - 1 \right) & x < 0. \end{cases} \tag{29}
$$

It has been shown to improve performance over ReLU and CReLU agents, particularly in environments with heavy input distribution shifts [22].

Concatenated ReLU (CReLU) Originally developed in the context of image classification, the CReLU activation function in Equation (30) concatenates the ReLU output with its negation [95]:

$$
\text{CReLU}(x) = \Big[\text{ReLU}(x), \text{ReLU}(-x) \Big] . \tag{30}
$$

Thus this activation function results in that subsequent layers have twice the number of input features, which requires care when comparing CReLU networks to regular ReLU networks. Regarding plasticity loss, Abbas et al. [1] apply CReLU to deep RL agents and observe three benefits. First, Rainbow + CReLU is able to change its parameters even late in training and after multiple task shifts. Second, CReLU improves gradient flow through the network and prevents gradient collapse. Third, CReLU effectively mitigates dead neurons because $\text{CReLU}(x) = 0$ if and only if $x = 0$ compared to ReLU, where $\text{ReLU}(x = 0)$ if $x \in (-\infty, 0]$.

Adaptive Rational Activations build on the fact that ratios of polynomials can approximate any continuous function. Denoting P and Q as two polynomials with input x, an adaptive rational activation is defined as

$$
\text{R}(x) = \frac{\text{P}(x)}{\text{Q}(x)} = \frac{\sum_{j=0}^{m} a_j x^j}{1 + \sum_{k=1}^{n} b_k x^k}, \tag{31}
$$

where $\{a_j\}_{j=0}^{m}$ and $\{b_k\}_{k=1}^{n}$ are $m + 1$ and n learnable parameters, respectively. Rational activations have two desirable properties from the perspective of plasticity loss, namely that they can adjust their parameters depending on input distribution shifts and that they can approximate residual connections. To stabilize them in practice, one uses the absolute sum in the denominator and sets $m = n + 1$ [22][7].

It seems clear that activation functions can help mitigate plasticity loss to some extent by reducing the number of dead units and improving gradient flow through the network. However, multiple experiments have shown that plasticity loss still occurs to varying levels with different activation functions [23, 97]. Therefore, we conclude that while choosing specific activation functions may alleviate the symptoms of plasticity loss, the activation function itself is not the root cause of the phenomenon.

---

7. Delfosse et al. [22] use $m = 5$ and $n = 4$ throughout their paper.

Activation functions

All activation functions below are defined for a scalar input $x \in \mathbb{R}$:

- **PELU** [35] is a variant of ELU with learnable slope parameters α and β parameters:

$$\text{PELU}(x) = \begin{cases} \frac{\alpha}{\beta} h & x \geq 0 \\ \alpha \left(e^{\frac{h}{\beta}} - 1 \right) & x < 0. \end{cases}$$

- **CReLU** [1, 95] concatenates the ReLU activation with its negation, which leads to twice the number of inputs at the subsequent layer but prevents dead neurons except for exactly zero pre-activations:

$$\text{CReLU}(x) = \left[\text{ReLU}(x), \text{ReLU}(-x) \right].$$

- **Adaptive rational activations** [22] use a ratio of polynomials with learnable coefficients a_j and β_k as activation function, allowing the activations to adapt to input distribution shifts:

$$\text{R}(x) = \frac{\text{P}(x)}{\text{Q}(x)} = \frac{\sum_{j=0}^{m} a_j x^j}{1 + \sum_{k=1}^{n} b_k x^k}.$$

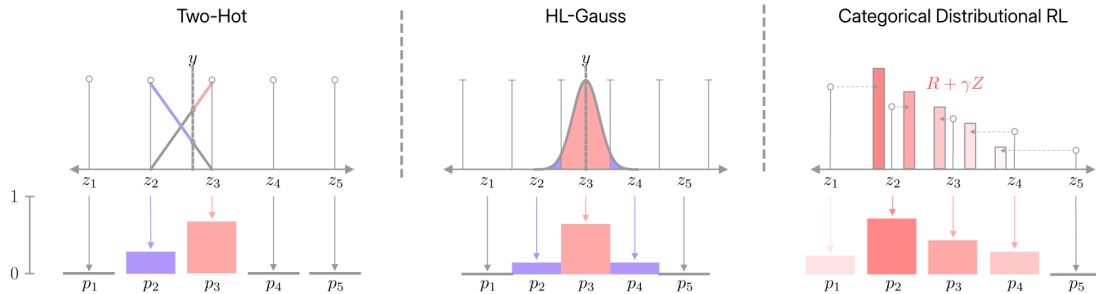---

6.6 Categorical Losses

Figure 3: **Visualization of categorical losses for deep RL**. The two-hot representation [93] proportionally assigns probability mass to the two neighboring bins of a scalar target y. HL-Gauss [49] constructs a Gaussian with fixed standard deviation and integrates over each bin to obtain the corresponding probability mass. Distribution RL algorithms such as C51 [8] model the full return distribution. Detailed descriptions of these methods are in Section 6.6. Figure taken from Farebrother et al. [29].

It is common knowledge among deep learning practitioners that it is easier to scale network sizes for classification tasks when compared to arbitrary regression tasks [8] [29, 49].

---

8. Image reconstruction using per-pixel regression side-steps common regression issues such as large errors and unstable gradients by exploiting the fact that pixel values are bounded. This enables the use of normalized objectives, which does not work for unbounded regression targets common in deep RL.

Even when regression is the actual task, re-formulating the learning problem using a cross-entropy loss is often beneficial [29, 49]. As explained in Sections 5.6 and 5.7, regression gradients are proportional to the loss, which in turn may lead to parameter norm growth. All categorical losses for deep RL have in common that they (a) require the rewards to be bounded to avoid distributions with infinite support, and (b) that the finite reward range is binned into M bins $(z_1, ..., z_M)$. Figure 3 visualizes three different approaches for discretizing regression targets in deep RL. Bounded rewards can usually be obtained by just clipping rewards within a range of $(-20, 20)$ [8]. One can then obtain a Categorical target distribution by either directly projecting a scalar target value y onto the bins [93] or by first constructing an auxiliary distribution $P(y|\mathbf{x})$ around y before the projection step [29]. In the following, we will present the three most popular approaches for converting regression into classification tasks used in deep RL.

Distributional RL (C-51) tries to estimate the full reward distribution instead of only its expected value [9]. C-51 [8], an early representative of distributional RL, projects the return distribution directly onto a categorical distribution with $M = 51$ bins, giving rise to its name. The authors justify this approach compared to using a continuous distribution with the advantages of the categorical distribution in terms of expressivity and computational efficiency. C-51 then minimizes the forward KL-divergence between the network's distribution $Z(\mathbf{s}, \mathbf{a}; \theta)$ and the target distribution $Z(\mathbf{s}, \mathbf{a}; \tilde{\theta})$ by using a cross-entropy loss:

$$L(\theta) = D_{KL}(Z(\mathbf{s}, \mathbf{a}; \theta) \parallel Z(\mathbf{s}, \mathbf{a}; \tilde{\theta})). \tag{32}$$

Subsequently, more modern distributional RL algorithms such as QR-DQN or IQN have refined the idea of modeling the return distribution and yielded large gains in sample efficiency [9]. While it is still elusive as to what exactly causes the performance benefits of distributional RL, recent work suggests that using a cross-entropy loss instead of regression might be one of the driving forces [29].

Two-hot Representations project a scalar-valued regression target $y \in \mathbb{R}$ onto a categorical distribution by proportionally assigning probability mass to the two closest bins around y. Concretely, for bin size one, the probability of the lower bin would be $P(\lfloor y \rfloor) = \lceil y \rceil - y$, whereas the probability of the higher bin would be the complementary probability $P(\lceil y \rceil) = 1 - P(\lfloor y \rfloor)$. All other bins are assigned zero probability mass. Using the binning strategy above, one can construct a categorical distribution that is usable as a target in a cross-entropy loss function. The scalar target y can then be recovered by taking the expectation of the corresponding categorical distribution. First popularized in the MuZero paper [93], the two-hot representation has since been noted to alleviate plasticity loss in multiple follow-up works, albeit at the cost of training stability [66, 68].

HL-Gauss uses two steps to project a scalar valued regression target $y \in \mathbb{R}$ onto a categorical distribution $Z(\mathbf{s}, \mathbf{a}; \tilde{\theta})$ with m bins $(z_1, ..., z_m)$ of width ζ. The target can be recovered as the expected value of the categorical distribution $y = \mathbb{E}[Z(\mathbf{s}, \mathbf{a}; \tilde{\theta})]$. In the first step of the projection, we construct a Gaussian distribution with mean y and a fixed variance σ^2: $\mathcal{N}(y, \sigma^2)$. Subsequently, we integrate over the Gaussian's density function in each bin z_i to obtain the corresponding probability mass p_i of the categorical distribution:

$$p_i(\mathbf{s}, \mathbf{a}; \tilde{\theta}) = \int_{z_i - \varsigma/2}^{z_i + \varsigma/2} f_{Y|\mathbf{s}, \mathbf{a}}(y \mid \mathbf{s}, \mathbf{a}) dy$$
$$= F_{Y|\mathbf{s}, \mathbf{a}}\left(z_i + \varsigma/2 \mid \mathbf{s}, \mathbf{a}\right) - F_{Y|\mathbf{s}, \mathbf{a}}\left(z_i - \varsigma/2 \mid \mathbf{s}, \mathbf{a}\right), \tag{33}$$

where $\tilde{\theta}$ are the target network parameters. HL-Gauss then uses a cross-entropy loss to optimize the agent's value function [29]. Compared to the two-hot representation, HL-Gauss improves performance in several settings and yields more expressive representations. The authors hypothesize that two effects are at play here: First, spreading the probability mass leads to reduced overfitting due to an effect akin to label smoothing in supervised learning. Second, HL-Gauss generalizes across ranges of target values by exploiting the ordinal structure of a regression problem [29].

6.7 Distillation

Distillation is a technique for transferring the knowledge of one network architecture to a different architecture by training a *student network* to predict the outputs of a *teacher network* [43]. However, it can also be used to reduce negative side effects occurring during the training of the teacher network.

ITER is a method for mitigating "*transient non-stationarity*" — another term for plasticity loss — occurring during network training [47]. It periodically distills the actor and critic networks of a PPO agent, showing that this mitigates plasticity loss in ProcGen and supervised toy experiments. To improve the computational efficiency of ITER, the authors propose to update the student networks in parallel with the teacher's RL training. This has the advantage of not requiring a replay buffer for on-policy algorithms such as PPO and enables parallel training of the teacher and student.

Hare & Tortoise Networks combine the intuition behind periodic weight resets with distillation by building on top of target networks. Specifically, they train a "*hare*" network to rapidly learn a new task via SGD. The "*tortoise*" network is a copy of the hare network that is updated using an exponential moving average of the hare's parameters [62]. This dual architecture is analogous to the hippocampus and neocortex in the brain, allowing the tortoise network to slowly integrate useful information from the hare network over the course of training. Instead of periodic hard resets or soft resets with uninformative initial parameters [5], the hare is reset to the tortoise's parameters. This enables frequent resetting without losing knowledge accumulated via SGD and even provides a mechanism for escaping suboptimal local minima via a hard reset of the hare [62].

6.8 Other Methods

In this section, we discuss methods relevant for plasticity loss that did not fit into one of the previous categories. Many of them are well-known regularization techniques such as LayerNorm [6] or data augmentations that were not designed to mitigate plasticity loss but also affect it.

Layer Normalization (LayerNorm)   [6] is a normalization scheme developed to address some limitations of Batch Normalization [50], namely removing its dependence on the batch size and enabling an application to recurrent neural networks. It does so by standardizing a network's lth layer's features using the per-layer activation statistics. In Equation (34), we will assume that LayerNorm is applied *before* the activation function of a layer, as is common in the literature [67, 68, 81]. Denoting $\mathbf{a}_l$ as the activations of layer l, LayerNorm performs a location-scale transformation to the standardized inputs with $\boldsymbol{\gamma}$ being a learnable scale parameter and $\boldsymbol{\beta}$ a learnable bias parameter:

$$\mathbf{a}_l \leftarrow \frac{\mathbf{a}_l - \mathbb{E}[\mathbf{a}_l]}{\sqrt{\mathrm{Var}[\mathbf{a}_l] + \epsilon}} \cdot \boldsymbol{\gamma} + \boldsymbol{\beta} \; . \tag{34}$$

$\epsilon > 0$ is a constant for improving numerical stability. LayerNorm first surfaced as a mitigation strategy for plasticity loss in the study of Lyle et al. [66], which found that it maintains network plasticity while only minimally affecting task performance. Many subsequent works have by now corroborated these results [67, 68, 80, 81].

But what exactly causes the performance gains of LayerNorm? First and most obviously, it does what it was supposed to do at conception and maintains zero-mean and unit-variance pre-activation statistics [6]. This is supposed to help with network training [68]. Lyle et al. [66] hypothesize that this is due to LayerNorm's ability to reduce gradient covariance. A study by Nauman et al. [80] finds that LayerNorm is very effective at mitigating overestimation bias, reducing dormant neurons [97], and preventing large gradient norms. Another answer is that pre-nonlinearity LayerNorm prevents unit linearization by stabilizing the pre-activation distribution [68]. This prevents divergence in value-based RL, which can also be achieved by using bounded activation functions [12]. Recently, Lyle et al. [67] studied the effects of LayerNorm on deep RL agents in-depth and identified two mechanisms behind its performance improvements in detail. First, LayerNorm is able to reactivate dead ReLU neurons by providing them with non-zero gradients from the normalization statistics. This is an effect that has also been observed by previous work [80]. In fact, studies with transformer networks have shown that the gradients from normalization statistics are the driving force behind LayerNorm's benefits [108] and not the zero-mean, unit-variance activations that were previously hypothesized [6, 67]. Second, LayerNorm induces an implicit, parameter-norm-dependent learning rate schedule that might be required for deep RL agents to learn certain behaviors [67].

Data Augmentations   have been the driving force behind impressive sample efficiency gains in pixel-based control. Conventional wisdom assumes that these gains are due to improved representation learning [60, 109, 110]. Ma et al. [69] challenge this assumption and provide evidence that data augmentations actually help prevent plasticity loss in the critic of a DrQ-v2 [110] agent. They support their hypothesis by measuring the fraction of active units, finding that including data augmentations prevents early plasticity loss as measured by a drop in the fraction of active units. Building on this insight, Ma et al. [69] propose to increase the number of gradient steps per environment step once the algorithm is past the early stage of plasticity loss.

Moment Resets   Asadi et al. [4] examine the effect of Adam moment accumulation in the context of value-based deep RL. As many of these methods use target networks, they

are effectively solving a sequence of optimization problems instead of a single problem with stationary targets. When examining the Adam moments directly after a target network update, Asadi et al. [4] find that the gradients for the new targets are orthogonal to the moments stored by Adam. As the moments update only slowly due to the typically high exponential smoothing coefficients β_1 and β_2, a target network update is followed by a lengthy phase of unlearning. Resetting the moments provides a simple solution to this issue [4].

Activation Normalization   p-norm is a normalization technique aiming to prevent saturated tanh units in continuous control actor networks [15]. It does so by dividing the features of the penultimate layer of the network $\phi(\mathbf{s})$ by their norm, i.e., $\phi_{\mathrm{norm}}(\mathbf{s}) = \frac{\phi(\mathbf{s})}{\|\phi(\mathbf{s})\|}$. Afterward, the actions are generated by a linear transformation of the normalized features $\phi_{\mathrm{norm}}(\mathbf{s})$, followed by a tanh activation function. While being developed specifically for the actor of DrQ-v2 [110], Bjorck et al. [15] also apply p-norm to the critic and find that regularizing both networks leads to substantially increased performance and training stability.

Discrete Representations   build on vector quantization techniques and have shown impressive results and a number of advantages when applied to generative models [101]. Meyer et al. [73] examine their effect in continual deep RL and discover they also have beneficial effects there. In particular, one-hot representations seem to learn more general representations that are able to adapt faster to non-stationarities in the environment. In their work, they hypothesize that the sparse and binary nature of the learned embeddings drives the performance benefits. This is verified by showing that one-hot representations substantially outperform quantized ones despite their identical information content [73].

Sharpness-Aware Minimization (SAM)   is an optimization technique for finding local minima with low curvature. Such flat minima are desirable because they are commonly associated with better generalization performance [31]. In the context of deep RL, Lyle et al. [66] hypothesize that the loss curvature as measured by the largest eigenvalue of the network's Hessian matrix might be an underlying driver of plasticity loss. SAM formulates finding a flat minimum as a minimax optimization problem, where it first has to find a set of "*adversarial*" weights θ_{adv} that maximally increase the loss $L(\theta_{\mathrm{adv}})$ within an ϵ-ball of radius ρ around the current parameters θ_t. As solving this problem exactly is costly, SAM uses a first-order Taylor expansion to find θ_{adv} by taking an ascending step along $\nabla_\theta L(\theta_t)$, with the step-size scaled to put θ_{adv} on the border of the ϵ-ball. We can then compute a gradient $\nabla_\theta L(\theta_{\mathrm{adv}})$ that moves in the direction of a loss region with uniformly flat value. SAM applies $\nabla_\theta L(\theta_{\mathrm{adv}})$ *at the current parameters θ_t* for its update. Together, these two steps can be seen as a perturbation step followed by an update step, forming an alternating optimization algorithm. SAM can increase plasticity even in pre-trained networks as it does not change the network architecture compared to other techniques such as LayerNorm. Its main disadvantage is that each update requires two gradient steps instead of just one, making it computationally more expensive than using SGD or momentum-based optimizers such as Adam [61].

6.9 Combined Methods

As the exact causes for plasticity loss are currently unclear and potentially multi-faceted [68], combining different approaches targeting specific symptoms of plasticity loss is a reasonable strategy. Many approaches, therefore, with the notable exception of Normalize-and-Project [67], have been introduced and discussed in previous sections. The box below provides a summary of particularly well-performing combinations.

Normalize-and-Project (NaP) combines LayerNorm with a regularization step similar to SpectralNorm. Concretely, given a desired target norm ρ, NaP regularizes the lth layer's parameters $\mathbf{W}$ to be within a ball of radius ρ [67]:

$$\mathbf{W}_l \leftarrow \rho \frac{\mathbf{W}_l}{\|\mathbf{W}_l\|} \tag{35}$$

Comparing Equation (35) with SpectralNorm, cf. Equation (21), we can observe that setting $\rho = 1$ and using the L2 norm recovers a variant of SpectralNorm.

Lyle et al. [67] proceed to note several important implementation details: First, linear layers now do not need a bias term, as LayerNorm already adds a learnable offset parameter. Second, an important question is how to handle these learnable parameters of LayerNorm in the projection step. The straightforward solution provided by Lyle et al. [67] aligns with previous research in supervised learning: Simply remove them, they are not relevant for LayerNorm's performance gains [108]. Nevertheless, the authors of NaP discuss several other options in their work. Lastly, adding a projection step to networks using LayerNorm removes its implicit, parameter-norm-dependent learning rate schedule. In the case of deep RL, this may require a custom learning rate schedule mimicking the one induced by LayerNorm. Lyle et al. [67] find that a simple linear decay proportional to the otherwise occurring parameter norm growth is sufficient.

Regularization Combinations

- **LayerNorm + L2 regularization** has been proposed by Lyle et al. [68], who were also the first to use LayerNorm to mitigate plasticity loss [66]. In this setup, LayerNorm prevents preactivation distribution shifts, and L2 regularization prevents parameter norm growth and gradient explosion.

- **Resets + L2 regularization** is a synergistic combination of regularization techniques found in the broad study by [80], which performs particularly well for SAC [39] on the Meta-World benchmark [111].

- **LayerNorm + Resets** has been shown to yield a large performance boost for SAC [39] on DeepMind control suite by the same authors [80].

- **BBF** is the state-of-the-art agent on Atari-100k. It employs a deeper network with residual blocks [41] based on the Impala-CNN architecture [28, 94]. To mitigate plasticity loss, BBF combines hard resets for the network head with soft resets for the ResNet encoder and uses weight decay for stable training with high replay ratios [80, 94].

- **PLASTIC** combines the CReLU activation function with sharpness-aware optimization, LayerNorm, and head resets for strong performance gains on Atari-200k and DeepMind control suite [61].

- **BRO** [81] is a state-of-the-art algorithm for proprioceptive continuous control tasks. From a plasticity perspective, it combines full network resets with LayerNorm and weight decay. Additionally, BRO uses a bespoke residual network, optimistic exploration, and a quantile network for the critic.

- **Normalize-and-Project (NaP)** combines LayerNorm with a version of Spectral-Norm, projecting the weights onto a ball with fixed radius ρ instead of the unit ball [67]:

$$\textit{Normalize}: \mathbf{a}_l \leftarrow \frac{\mathbf{a}_l - \mathbb{E}[\mathbf{a}_l]}{\sqrt{\text{Var}[\mathbf{a}_l] + \epsilon}} \cdot \boldsymbol{\gamma} + \boldsymbol{\beta} \; ; \quad \textit{Project}: \mathbf{W}_l \leftarrow \rho \frac{\mathbf{W}_l}{\|\mathbf{W}_l\|}$$

When implementing NaP, the scale and offset parameters of LayerNorm can often be removed [67, 108].

6.10 Discussion of Mitigation Strategies

One thing stands out when looking at the strategies currently proposed to mitigate plasticity loss: Many of them "treat" a particular pathology of plasticity loss, similarly to how medication against a headache treats that particular symptom of an underlying disease. Recalling the findings of Section 5, this is rather unsurprising, as we still lack a deeper understanding of what causes plasticity loss.

Similarly, we do not have a deep understanding of most mechanisms behind the performance gains. For example, LayerNorm's performance benefits have been attributed to its ability to maintain zero-mean and unit-variance pre-activations [6], when in reality, it seems to be the case that it effectively prevents dead units [108] and induces an advantageous learning rate schedule [67]. Similarly, recent insights into BatchNorm [50] have shown that it can effectively regularize a Q-function such that target networks are superfluous [12], but at the same time, BatchNorm also makes agents myopic [34].

In Table 2, we provide an overview of causes and mitigation strategies for plasticity loss. Given the state of research, it is no surprise that current SOTA methods often combine multiple regularizers, each treating an individual aspect of plasticity loss. For example, PLASTIC employs the SAM optimizer and LayerNorm to deal with the loss of input plasticity and uses resets combined with the CReLU activation function to improve target plasticity [61]. BRO [81] and BBF [94] are agents in a similar vein, as they both use multiple regularizers to successfully mitigate plasticity loss and improve sample efficiency.

Table 2: **Overview of causes and mitigation strategies for plasticity loss.**
Causes: Saturated Units (SU) , Rank Collapse (RC) , First-Order Effects (FOE) , Second-Order Effects (SOE) , Non-stationarity (NS) , Regression loss (RE) , Parameter Norm Growth (PNG) , high replay ratios (RR) , and Early Overfitting (EO) .
Mitigation Strategies: Non-targeted Weight Resets (NW) , Targeted Weight Resets (TW) , Parameter Regularization (PR) , Feature Rank Regularization (FR) , Activation Functions (AF) , Categorical Loss (CL) , Distillation (DI) , LayerNorm (LN) , Moment Resets (MR) . Methods that just occur once, e.g., data augmentation, are spelled out.

Name	Causes	Mitigation Strategies
p-norm [15]	SU	p-norm
Plasticity Injection [83]	NS	TW
UPGD [26]	SU , NS	TW
Continual Backprop [23]	SU , NS	TW , MR
ReDo [97]	SU , NS	TW , MR
"Resetting the optimizer" [4]	FOE	MR
DrM [107]	–	NW
Primacy Bias [82]	RR , EO	NW
SR-SAC [25]	RR ; EO	NW
PLASTIC [61]	NS , SOE	NW , LN , AF , SAM opt.
BBF [94]	–	NW , PR
"Bitter lesson" [80]	SU , FOE , PNG , RR	NW , PR , LN
BRO [81]	–	NW , PR , LN , CL
L2 Init [24]	NS	PR
Deeper deep RL [14]	FOE , deep networks	PR
SpectralNorm for RL [36]	FOE	PR
"Disentangling Plasticity" [68]	NS , RE , FOE , SU , PNG	PR , LN
Normalize-and-Project [67]	PNG , SU , FOE , lr schedule	PR , LN
Weight Clipping [27]	NS , PNG , FOE	PR
Wasserstein Regularizer [63]	SOE	PR
"Understanding plasticity" [66]	NS , FOE , SOE , RE	PR , LN , CL
HL-Gauss [29, 49]	RE , NS	CL
SAM optimizer [31]	SOE , label noise	SAM optimizer
Discrete representations [73]	NS , continuous representations	one-hot quantized representation
"Revisiting Plasticity" [69]	NS , RR	Data aug., RR scaling
Singular value reg. [56]	RC , NS	FR
InFeR [65]	RC , NS	FR
DR3 [57]	RC ,	FR
BEER [42]	RC , FOE	FR
Reg. in offline RL [38]	RC , SU	FR
ITER [47]	NS	DI
Hare & Tortoise [62]	NS	DI
CReLU [1]	NS , FOE	AF
PELU [35]	–	AF
Rational Activations [22]	NS , overestimation	AF

7. Factors Influencing Plasticity Loss

This section provides a brief overview of factors affecting plasticity loss when training deep RL agents. While there is some overlap with previous sections, the focus here is on providing practical insights and hyperparameter settings that are easy to use and do not require domain-specific expertise in plasticity loss. An example of this is the choice of the value of ϵ in Adam.

Non-stationarity Section 5.5 discusses different types of non-stationarity as possible causes of plasticity loss. Clearly, the presence, type, and extent of non-stationarity have an influence on networks losing plasticity. How this can be quantified and used to strategically deploy specific remedies is currently not yet determined. The extent of target non-stationarity seems to play a clear role in plasticity loss [47, 97], but whether input non-stationarity plays a similarly important role or not is not yet clear [61, 97]. For example, offline RL seems less affected than online RL [97]. In supervised learning, task shifts are causing plasticity loss to some extent [5, 10] but the severity of this loss depends on how different the tasks are—which is difficult to quantify. In deep RL, a change in the dynamics of an MDP is associated with plasticity loss [1]. Given that agents employing TD learning implicitly learn about an MDP's transition function, it seems likely that their learning ability suffers more from dynamics changes compared to other types of RL algorithms [64].

Activation Function The choice of activation function can substantially affect loss of plasticity, mainly due to its effects on gradient propagation. Clearly, ReLU's susceptibility to dead neurons throughout training may contribute to plasticity loss. Using alternative activation functions has been shown to work well under non-stationarity, e.g., using CReLU [1] or rational activations [22] often improves performance. However, choosing the "correct" activation function is no panacea: LeakyReLU should be less prone to dead neurons but still suffers from plasticity loss [97], maybe due to linearized units [68] or unbounded activations [12]. And while TanH nonlinearities guarantee bounded activations, they can still saturate, reducing performance [15]. Above all, not all activation functions may lead to the same task performance, requiring trade-offs to be made [23].

Optimizer The choice of optimizer, particularly when it uses moments for its updates, can impact plasticity loss. Adam, commonly used in deep RL, uses the following update rule [54]:

$$u_t = \alpha \frac{\hat{m}_t}{\sqrt{\hat{v}_t} + \epsilon}, \tag{36}$$

where α is the learning rate, $m_t = \beta_1 m_{t-1} + (1 - \beta_1) \nabla_\theta f(\theta_{\theta_t})$ is an exponential moving average of the first moment, and $\hat{m}_t = m_t/(1 - \beta_1^t)$ its bias-corrected version. For the second moment, $v_t = \beta_2 v_{t-1} + (1 - \beta_2) (\nabla_\theta f(\theta_{\theta_t}))^2$ and $\hat{v}_t = v_t/(1 - \beta_2^t)$ are the analogous quantities. $\epsilon > 0$ is a constant added for numerical stability.

In deep RL, the magnitude of Adam's gradient update can explode because of $\hat{m}_t$ being updated more aggressively than $\hat{v}_t$ due to $\beta_2 > \beta_1$ [9]. To see why this occurs, let us consider the case of DQNs with target networks. After a target network update, the agent has to

---

9. For example, the default values in Pytorch are $\beta_1 = 0.9$ and $\beta_2 = 0.999$ [90].

solve a new, slightly different regression task [4]. This results in larger errors due to the target change. These large errors then proportionally increase gradient norms in regression problems [66]. If we assume $\beta_2 > \beta_1$, then the magnitude of $\hat{m}_t$ may grow faster than the magnitude of $\hat{v}_t$ due to the more aggressive updates. Consequently, the training may diverge. Additionally, the ubiquitous use of target networks in value-based deep RL means that after a target update, the moments are not aligned with the current optimization objective. This can manifest in gradients being orthogonal to the current moment estimates and might require several updates to wear off. A remedy is resetting the moments after each target network update [4].

An especially interesting case in Adam is the numerical stability hyperparameter ϵ. In deep RL, it has become best practice to deviate from the low default values used in current frameworks [10], opting for higher values instead. For example, Google's dopamine framework uses a default of $1.5 \cdot 10^{-4}$, a value larger by 3 magnitudes [17]. This helps to prevent Adam's moment estimates from diverging in the presence of task shifts, e.g., when the target networks are being updated.

Optimization Hyperparameters   We now briefly review some optimization hyperparameters that likely have an effect on plasticity loss. These are the learning rate, the total number of training steps, and the batch size. In supervised learning, larger learning rates may help to escape suboptimal local minima when fine-tuning from a pretrained network [10]. In offline deep RL, on the other hand, using high learning rates is prone to result in rank collapse and an increase in dead neurons [38]. Additionally, Lyle et al. [67] have shown recently that implicit learning rate scheduling may play a more prominent role in deep RL than previously thought. Much work is left to understand the interplay between learning rate and plasticity loss. Still, it seems clear that properly tuning the learning rate can help prevent catastrophic loss of plasticity, mainly when using adaptive optimizers such as Adam [38, 66].

Another parameter affecting plasticity loss is the total update budget. Intuitively, the longer a network is trained on one task before shifting to the next, the more likely it is to lose plasticity [63].

Lastly, the batch size may affect plasticity loss as well. There are conflicting reports in this regard: Obando-Ceron et al. [84] find improved results when using smaller batch sizes for a distributional RL agent on Atari, likely due to less gradient collinearity arising from more noisy gradients. However, in offline deep RL, using larger batch sizes allows for maintaining strong performance even with larger learning rates, whereas smaller batch sizes are associated with dead units [38]. Nauman et al. [81] build on a SAC [39] agent and find that lower learning rates work better to scale online continuous control, again in line with the previously mentioned Atari results [84]. Therefore, we advise manually tuning the batch size for the specific task and environment.

Regularization   Many commonly used regularizers from supervised deep learning affect plasticity [80]. LayerNorm and SpectralNorm may be very effective at preventing gradient explosion, particularly when training with high replay ratios [80]. Recently, Lyle et al. [67] have shed light on how LayerNorm can even prevent dead or dormant units by providing

---

10. For example, Pytorch uses a default value of 10^{-8}.

gradients from its normalization statistics [108]. Both SpectralNorm and LayerNorm also significantly reduce overestimation bias in SAC agents [80]. L2 regularization prevents parameter norm growth, which is hypothesized to be one of the main drivers of plasticity loss [27, 68]. Unsurprisingly, it is therefore used in the current SOTA agents for Atari-100k [94] and proprioceptive continuous control [81]. The usage of BatchNorm [50] in deep RL agents is less common despite generalization benefits [21], likely because integration into target networks is non-trivial [12]. An advantage of the well-established regularizers mentioned above over domain-specific methods [27, 63] is that they are broadly tested and efficiently implemented in common deep learning frameworks such as Pytorch [90]. As of now, it is still an open question whether other regularization techniques may help with plasticity loss and whether they may be able to alleviate other issues apart from overestimation bias.

Objective Function   As regression losses are less amenable to neural network optimization than classification losses [29], it appears reasonable to use cross-entropy losses as default. Having gradients proportional to error magnitude seems to contribute to several pathologies associated with plasticity loss, such as large gradients and growing parameter norms. However, it is not entirely clear which type of categorical loss is best for which problem. For example, HL-Gauss yields great results when applied to DQN [75] or CQL agents [55] in discrete-control environments. For continuous control, Nauman et al. [81] found implicit quantile networks [9] to be superior to alternative objectives for SAC agents [39]. While trying out different loss reformulations is sensible, there is no conclusive evidence of one being consistently better than the others.

Network Architecture   Compared with supervised learning, most deep RL agents have a somewhat peculiar architecture: For proprioceptive control tasks, their networks are usually small MLPs, especially when compared with modern deep networks [29, 81]. For pixel-based control tasks, many algorithms still build on top of the CNN architecture presented in the original DQN paper [75]. For example, SR-SPR still uses the same CNN trunk as the one used in DQN [25]. Recently, more modern algorithms have used ResNet-style architectures [81, 94] to scale up the agent networks. However, the field of deep RL is still only at the beginning of utilizing large-scale networks, with the number of parameters peaking at $\approx 80M$ due to optimization issues [29]. This is despite findings that bigger agents may be more robust to plasticity loss [65, 66]. Particularly, network width can somewhat alleviate plasticity loss, although even very wide networks cannot completely mitigate it [66]. Deeper networks, on the other hand, do not seem to be able to mitigate plasticity loss. A successful strategy for increasing the network sizes in deep RL might be to use residual architectures in conjunction with commonly used deep learning regularization such as LayerNorm, SpectralNorm, or L2 regularization [81, 94].

Environment Properties   Deep RL environments are diverse in nature and some of the properties of specific environments appear to exacerbate plasticity loss. For Atari, different games possess different levels of input non-stationarity. Delfosse et al. [22] accordingly classify games into the categories *stationary*, *dynamic*, and *progressive* environments. In stationary environments, the input distribution doesn't change at all. Dynamic environments have shifts in their input distribution, occurring independently of the current policy. An example is the game Asterix, where the agent receives gear such as a helmet as the game

progresses. Progressive environments differ from dynamic environments because the input distribution shifts depend on the current policy. A typical environment in this category is JamesBond, where the agent progresses to levels with different characteristics [22]. In continuous control, particularly in the DeepMind control suite Tassa et al. [99], the action dimension also plays a crucial role in plasticity loss. DOG and Humanoid are notoriously difficult benchmarks due to the agent having to control many different joints simultaneously. When training agents in these environments, the large number of dimensions in the action space leads to diverging gradients for the critic, and networks quickly lose plasticity [80]. These different environment properties, e.g., DM Control and MetaWorld, lead to inconsistent performance gains for different regularizers [80].

8. Current State and Future Directions

In this section, we first discuss current trends in research on plasticity loss, followed by suggestions for future research.

8.1 Current Trends

Regarding potential causes of plasticity loss, the field has come a long way in the last few years. Compared to simply noting training instabilities [75] or gradient issues [14], we now have a much deeper understanding of which factors of plasticity loss might cause which pathologies. An example is large-mean regression causing exploding parameter norms, which in turn causes sharpness in the optimization landscape [68].

Stepping back and trying to distill trends in the field, we notice that well-established regularizers such as LayerNorm, BatchNorm, or weight decay are more commonly used to deal with plasticity loss in particular, but also other deep RL optimization issues such as overestimation bias [34, 81, 94]. The reason for this is that they're easy to implement, efficient to compute, and usually have few hyperparameters. In contrast, customized variants of SGD that require expensive tracking of various metrics on top of a myriad of hyperparameters are rarely used in SOTA agents.

In conclusion, there seems to be a "bitter lesson" of plasticity loss: General network regularization will prevail over domain-specific methods purely targeting plasticity loss. A similar observation has recently been made regarding overestimation bias, where it has been found that general network regularizers such as LayerNorm are often more effective at preventing overestimation than domain-specific pessimistic learning algorithms [80].

As a community, we are progressing towards a theoretical understanding of causes and remedies of plasticity loss [34]. Regarding the empirical research in the field, recent advances in just-in-time compilation [16] and GPU-accelerated environments [32, 59] enable scaling up experiments. These more efficient approaches will likely accelerate research on plasticity loss, just as they will generally accelerate research in deep RL.

8.2 Directions for Future Research

8.2.1 WHAT ARE THE CAUSES BEHIND PLASTICITY LOSS?

The causal relationships between different aspects and pathologies in plasticity loss are not yet fully understood. Non-stationarity likely plays a role [47, 62, 68], but how different types

of non-stationarity interact with different optimization problems remains unclear. Dividing non-stationarity into different aspects and examining them separately has yielded some progress [61, 62]. However, it is still challenging to quantify the extent of non-stationarity caused by, for example, a deep RL environment. Making progress in this area would make it possible to determine the strength of regularization based on the level of non-stationarity of the optimization problem. This is an exciting direction for future work due to many of the methods tackling plasticity loss interfering with solving the task [66].

Looking closer at the learning problem itself, a growing body of evidence hints at regression losses causing parameter norm growth, which in turn results in many of the commonly observed pathologies of networks that lost their plasticity [29, 68]. Large-mean regression can exacerbate this issue [68]. However, plasticity loss is also an issue for non-stationary classification, if maybe not to the same extent as for regression problems [47, 68]. Trying to develop causal relationships between different factors and symptoms of plasticity loss would allow a more fundamental understanding of the problem and make developing regularizers that interfere less with task optimization easier.

Lastly, it is clear that the initialization weights are more amenable to optimization. This fact is used by some methods to regularize the parameters towards their initial values or initial distribution during training [24, 63]. But what exactly makes the initial weights so good for learning? It seems that zero-mean, unit-variance pre-activations are helpful [67], but are there other factors at play? By borrowing from the extensive literature on neural network initialization, it might be possible to arrive at definitive properties that are necessary to maintain the learning ability of an agent.

To summarize, arriving at a more abstract conceptual understanding that connects different facets of plasticity loss is the most pressing area for future research. While recent studies have made substantial progress in this respect [66, 68, 80], a "grand theory" of plasticity loss is not yet in sight.

8.2.2 A CALL FOR BROADER EVALUATION

Section 7 mentions environment properties as one of the possible relevant factors for plasticity loss. Nauman et al. [80] confirm this hypothesis to the extent that different environments seem to suffer from lost plasticity to a different extent and that different pathologies occur at different levels of severity. For example, in DM Control DOG, large gradient norms pose a substantial optimization challenge to SAC agents. On other environments in DM Control, these large-norm gradients don't occur [80, 99]. Similarly, large parameter norms seem to harm agent performance on Metaworld [111] but do not affect the DM Control environments [80]. These effects result in fluctuating performance between different regularizers on different benchmarks. For example, while LayerNorm is highly useful for DM Control DOG, it does not improve performance for small networks on MetaWorld [80].

Here, the GPU-accelerated environment suites mentioned previously provide a unique opportunity for broadening our understanding of plasticity loss. What types of agents suffer the most from it? In which environments does it occur most severely? Developing abstract, measurable properties of environments that are associated with plasticity loss would dramatically help to build a more coherent understanding of the phenomenon. Additionally, it would allow deploying specific regularizers based on how strong the target environment

causes plasticity loss, enabling more targeted mitigation of the phenomenon for practitioners. Lastly, it would enable testing whether some regularizers have unintended side effects and how harmful these are. For example, it is well-known that LayerNorm makes a network input scale-invariant, mapping $\alpha\mathbf{x}$ and $\mathbf{x}$ to the same output [67]. This could lead to potentially harmful state aliasing, e.g., by mixing Euclidean coordinates.

8.2.3 How do well-known regularizers actually work?

State-of-the-art agents currently deploy a range of well-known regularization techniques from deep learning, such as LayerNorm [81], L2 regularization [81, 94], or BatchNorm [12]. But how exactly these interact with deep RL objectives and what the mechanisms driving their improvements are is not very well understood, from an empirical and a theoretical perspective.

On the empirical side, there is growing consensus that applying LayerNorm to deep RL agents is beneficial [68, 80]. Whether these benefits are due to LayerNorm maintaining zero-mean, unit-variance pre-activations [67], or due to it preventing dead neurons through gradients from normalization statistics [67, 108], or due to it centering and scaling gradients, or whether it is all of the above [108]: We currently do not yet know. Similar analyses can likely be made for other standard regularization techniques such as SpectralNorm.

Theoretically, these regularizers might have implicit effects on the RL formalism. For example, Bhatt et al. [12] use batch normalization to remove the need for a target network. This yields substantial performance gains for the standard, dense-reward continuous control tasks from DM Control. However, later work has shown that under mild assumptions, this provably leads to myopic behavior in linear agents with growing batch sizes [34]. Whether this is a problem in practice that outweighs the potential benefits of BatchNorm is still very much unclear.

8.2.4 What are the Links between Plasticity Loss and Established Deep RL Issues?

Overestimation bias is an issue plaguing any algorithm of the Q-Learning family: Because the argmax over Q-values uses the same network to select the target action and obtain the corresponding Q-value, the noise in both processes is correlated, leading to overestimation bias [98]. This issue has spawned many domain-specific solutions, ranging from classical double Q-Learning [102] to more recent approaches specifically targeting deep RL such as Generalized Pessimism Learning [18]. Are these domain-specific approaches really the best way to tackle overestimation bias? Recent work in plasticity loss suggests, in fact, a negative answer. In a broad study, Nauman et al. [80] find that well-known network regularization techniques such as LayerNorm [6] or SpectralNorm [74] are far superior at mitigating overestimation bias than GPL or commonly used clipped double Q-learning (CDQ). Removing CDQ is actually one of the most performance-critical components of the current SOTA algorithm for proprioceptive control [81]. Other works also connect plasticity loss and overestimation bias [22].

Similar stories can be found for other algorithmic components. For instance, ϵ-greedy exploration appears unnecessary in some deep RL applications because an optimization artifact called *policy churn* is actually driving exploration [92] by causing action changes in

a substantial amount of states through single gradient updates. Baird's counterexample [48] can easily be solved by modern, regularized Q-Learning even though function approximation should provably diverge [34]. Target networks as a stabilization technique can be made obsolete by proper regularization [12, 34], vastly improving the computational efficiency of Q-learning algorithms. These examples highlight a crucial insight: **Intuitions from tabular RL often do not transfer directly to deep RL and may even be harmful to understanding**.

What other potential discoveries lie at the intersection between RL, deep network optimization, and regularization? Section 8.2.5 provides an outlook from an exploration perspective. Many stabilizing hacks used in current algorithms, such as replay buffers, pessimism, or target networks, may prove unnecessary once we correctly understand the interplay between deep network training and RL [34, 81]. Looking at issues like the deadly triad [103] or the phenomenon of passive learning [89] from an up-to-date network optimization and regularization perspective is an intriguing direction for future work. Deep RL is learning its bitter lesson [80]: Over-engineered, domain-specific approaches are being replaced by general neural network regularizers.

8.2.5 Plasticity, Agent Behavior, and Exploration

Modern neuroscience has made great strides in linking patterns of neuronal activity to certain behaviors, moods, and feelings. In contrast, deep learning and deep RL, in particular, are only at the beginning of establishing links between agent behavior and neuron activity, making this an exciting direction for future research. In a seminal work, Xu et al. [107] have connected the phenomenon of neuron dormancy [97] with reduced activity in pixel-based continuous control agents. Resetting these neurons causes immobile agents to "*activate*" and move around in the environment. In the future, one could envision exploration algorithms that modulate specific neurons in the network, causing the agent to explore its environment in a more directed fashion compared to current approaches. In exploration terms, this would be called *deep* exploration, which refers to coherent long-term exploratory behaviors. In contrast, *dithering* algorithms such as ϵ-greedy cannot create long-term strategies and therefore struggle with hard exploration problems [87].

Another avenue is to investigate the success of current algorithms through a lens of plasticity. Schaul et al. [92] have recently shown that exploratory behavior of DQN agents is not due to ϵ-greedy as previously assumed, but instead depends on the agent's frequent action changes due to neural network optimization, a phenomenon coined *policy churn*. While they did not consider plasticity in their work, it is reasonable to assume that when networks lose their ability to learn, this also affects policy churn and, in turn, an agent's ability to explore.

Lastly, regularizing and mitigating plasticity loss has side effects that may allow the design of more efficient algorithms in general. One such example is clipped double Q-Learning, which has been an integral component in many foundational continuous control algorithms [33, 39]. Recently, it has been shown that this pessimistic bias is actually harmful to exploration, hurting the sample efficiency of these agents [79]. By applying insights from plasticity loss and proper regularization to these agents, it is possible to improve

exploration without suffering from overestimation bias, vastly improving the performance of these agents [81].

9. Conclusion

While many modern, sample-efficient RL algorithms must address the problem of plasticity loss, it has only recently gained broader attention as an explicit phenomenon of interest within the field of deep RL. With this survey, we aim to summarize the current state of the field and provide a starting point for aspiring researchers. To this end, we present a unified definition of plasticity loss and use it to examine relationships between different definitions considered in recent works. Furthermore, we offer a taxonomy of possible causes of plasticity loss and mitigation strategies in the literature. The following overview of factors influencing plasticity loss can be seen as a cookbook of tricks and hyperparameter settings currently used to mitigate plasticity loss. Lastly, we want to highlight a collection of issues and possible research directions we have identified in recent works:

- Section 5, Section 6, and Section 8.2.1: Focusing on specific, measurable pathologies of neural networks that have lost plasticity has resulted in improved algorithms but may divert attention from identifying underlying causes such as environment properties.

- Section 8.2.2 and Section 8.2.3: A broader evaluation beyond environments like Atari or DeepMind Control is necessary to ensure that algorithms robustly mitigate plasticity loss, how currently proposed mitigation strategies work "in the wild", and generate insights into why plasticity loss occurs in the first place.

- Section 8.2.5: Connections between the neural activation patterns of RL agents and their behavior are likely to yield insights that will enable the development of more efficient and principled algorithms.

We hope that this survey will be helpful for prospective researchers planning to work on plasticity loss and that it will provide a starting point for identifying relevant open problems.

Acknowledgments

References

[1] Zaheer Abbas, Rosie Zhao, Joseph Modayil, Adam White, and Marlos C. Machado. Loss of plasticity in continual deep reinforcement learning. In *Conference on Lifelong Learning Agents (CoLLAs)*, pages 620–636, 2023.

[2] David Abel, André Barreto, Benjamin Van Roy, Doina Precup, Hado Philip van Hasselt, and Satinder Singh. A definition of continual reinforcement learning. In

Alice Oh, Tristan Naumann, Amir Globerson, Kate Saenko, Moritz Hardt, and Sergey Levine, editors, *Advances in Neural Information Processing Systems (NeurIPS)*, 2023.

[3] Kai Arulkumaran, Marc Peter Deisenroth, Miles Brundage, and Anil Anthony Bharath. A brief survey of deep reinforcement learning. *CoRR*, abs/1708.05866, 2017.

[4] Kavosh Asadi, Rasool Fakoor, and Shoham Sabach. Resetting the optimizer in deep RL: an empirical study. In *Advances in Neural Information Processing Systems (NeurIPS)*, 2023.

[5] Jordan T. Ash and Ryan P. Adams. On warm-starting neural network training. In *Advances in Neural Information Processing Systems (NeurIPS)*, 2020.

[6] Lei Jimmy Ba, Jamie Ryan Kiros, and Geoffrey E. Hinton. Layer normalization. *CoRR*, abs/1607.06450, 2016.

[7] Marc G. Bellemare, Yavar Naddaf, Joel Veness, and Michael Bowling. The arcade learning environment: An evaluation platform for general agents. *J. Artif. Intell. Res.*, 47:253–279, 2013.

[8] Marc G. Bellemare, Will Dabney, and Rémi Munos. A distributional perspective on reinforcement learning. In *International Conference on Machine Learning (ICML)*, volume 70, pages 449–458, 2017.

[9] Marc G. Bellemare, Will Dabney, and Mark Rowland. *Distributional Reinforcement Learning*. MIT Press, 2023. `http://www.distributional-rl.org`.

[10] Tudor Berariu, Wojciech Czarnecki, Soham De, Jörg Bornschein, Samuel L. Smith, Razvan Pascanu, and Claudia Clopath. A study on the plasticity of neural networks. *CoRR*, abs/2106.00042, 2021.

[11] Christopher Berner, Greg Brockman, Brooke Chan, Vicki Cheung, Przemyslaw Debiak, Christy Dennison, David Farhi, Quirin Fischer, Shariq Hashme, Christopher Hesse, Rafal Józefowicz, Scott Gray, Catherine Olsson, Jakub Pachocki, Michael Petrov, Henrique Pondé de Oliveira Pinto, Jonathan Raiman, Tim Salimans, Jeremy Schlatter, Jonas Schneider, Szymon Sidor, Ilya Sutskever, Jie Tang, Filip Wolski, and Susan Zhang. Dota 2 with large scale deep reinforcement learning. *CoRR*, abs/1912.06680, 2019.

[12] Aditya Bhatt, Daniel Palenicek, Boris Belousov, Max Argus, Artemij Amiranashvili, Thomas Brox, and Jan Peters. Crossq: Batch normalization in deep reinforcement learning for greater sample efficiency and simplicity. In *International Conference on Learning Representations (ICLR)*, 2024.

[13] Celeste Biever. Chatgpt broke the turing test-the race is on for new ways to assess ai. *Nature*, 619(7971):686–689, 2023.

[14] Johan Bjorck, Carla P. Gomes, and Kilian Q. Weinberger. Towards deeper deep reinforcement learning with spectral normalization, 2021.

[15] Johan Bjorck, Carla P. Gomes, and Kilian Q. Weinberger. Is High Variance Unavoidable in RL? A Case Study in Continuous Control. In *International Conference on Learning Representations (ICLR)*. OpenReview.net, 2022.

[16] James Bradbury, Roy Frostig, Peter Hawkins, Matthew James Johnson, Chris Leary, Dougal Maclaurin, George Necula, Adam Paszke, Jake VanderPlas, Skye Wanderman-Milne, and Qiao Zhang. JAX: composable transformations of Python+NumPy programs, 2018.

[17] Pablo Samuel Castro, Subhodeep Moitra, Carles Gelada, Saurabh Kumar, and Marc G. Bellemare. Dopamine: A research framework for deep reinforcement learning. *CoRR*, abs/1812.06110, 2018.

[18] Edoardo Cetin and Oya Çeliktutan. Learning pessimism for reinforcement learning. In Brian Williams, Yiling Chen, and Jennifer Neville, editors, *Conference on Artificial Intelligence (AAAI)*, pages 6971–6979. AAAI Press, 2023.

[19] Xinyue Chen, Che Wang, Zijian Zhou, and Keith W. Ross. Randomized ensembled double q-learning: Learning fast without a model. In *International Conference on Learning Representations (ICLR)*. OpenReview.net, 2021.

[20] Djork-Arné Clevert, Thomas Unterthiner, and Sepp Hochreiter. Fast and accurate deep network learning by exponential linear units (elus). In Yoshua Bengio and Yann LeCun, editors, *International Conference on Learning Representations (ICLR)*, 2016.

[21] Karl Cobbe, Oleg Klimov, Christopher Hesse, Taehoon Kim, and John Schulman. Quantifying generalization in reinforcement learning. In Kamalika Chaudhuri and Ruslan Salakhutdinov, editors, *International Conference on Machine Learning (ICML)*, volume 97 of *Proceedings of Machine Learning Research*, pages 1282–1289. PMLR, 2019.

[22] Quentin Delfosse, Patrick Schramowski, Martin Mundt, Alejandro Molina, and Kristian Kersting. Adaptive rational activations to boost deep reinforcement learning. In *International Conference on Learning Representations (ICLR)*. OpenReview.net, 2024.

[23] Shibhansh Dohare, J. Fernando Hernandez-Garcia, Parash Rahman, Richard S. Sutton, and A. Rupam Mahmood. Maintaining plasticity in deep continual learning. *CoRR*, abs/2306.13812, 2023.

[24] Shibhansh Dohare, J. Fernando Hernandez-Garcia, Parash Rahman, Richard S. Sutton, and A. Rupam Mahmood. Maintaining plasticity in deep continual learning. *CoRR*, abs/2306.13812, 2023.

[25] Pierluca D'Oro, Max Schwarzer, Evgenii Nikishin, Pierre-Luc Bacon, Marc G. Bellemare, and Aaron C. Courville. Sample-efficient reinforcement learning by breaking the replay ratio barrier. In *International Conference on Learning Representations (ICLR)*. OpenReview.net, 2023.

[26] Mohamed Elsayed and A. Rupam Mahmood. Addressing loss of plasticity and catastrophic forgetting in continual learning. In *International Conference on Learning Representations (ICLR)*, 2024.

[27] Mohamed Elsayed, Qingfeng Lan, Clare Lyle, and A. Rupam Mahmood. Weight clipping for deep continual and reinforcement learning. *CoRR*, abs/2407.01704, 2024.

[28] Lasse Espeholt, Hubert Soyer, Rémi Munos, Karen Simonyan, Volodymyr Mnih, Tom Ward, Yotam Doron, Vlad Firoiu, Tim Harley, Iain Dunning, Shane Legg, and Koray Kavukcuoglu. IMPALA: Scalable Distributed Deep-RL with Importance Weighted Actor-Learner Architectures. In *International Conference on Machine Learning (ICML)*, pages 1406–1415, 2018.

[29] Jesse Farebrother, Jordi Orbay, Quan Vuong, Adrien Ali Taïga, Yevgen Chebotar, Ted Xiao, Alex Irpan, Sergey Levine, Pablo Samuel Castro, Aleksandra Faust, Aviral Kumar, and Rishabh Agarwal. Stop regressing: Training value functions via classification for scalable deep RL. In *International Conference on Machine Learning (ICML)*, 2024.

[30] Alhussein Fawzi, Matej Balog, Aja Huang, Thomas Hubert, Bernardino Romera-Paredes, Mohammadamin Barekatain, Alexander Novikov, Francisco J. R. Ruiz, Julian Schrittwieser, Grzegorz Swirszcz, David Silver, Demis Hassabis, and Pushmeet Kohli. Discovering faster matrix multiplication algorithms with reinforcement learning. *Nat.*, 610(7930):47–53, 2022.

[31] Pierre Foret, Ariel Kleiner, Hossein Mobahi, and Behnam Neyshabur. Sharpness-aware minimization for efficiently improving generalization. In *International Conference on Learning Representations (ICLR)*, 2021.

[32] C. Daniel Freeman, Erik Frey, Anton Raichuk, Sertan Girgin, Igor Mordatch, and Olivier Bachem. Brax - a differentiable physics engine for large scale rigid body simulation, 2021.

[33] Scott Fujimoto, Herke van Hoof, and David Meger. Addressing function approximation error in actor-critic methods. In *International Conference on Machine Learning (ICML)*, pages 1582–1591, 2018.

[34] Matteo Gallici, Mattie Fellows, Benjamin Ellis, Bartomeu Pou, Ivan Masmitja, Jakob Nicolaus Foerster, and Mario Martin. Simplifying deep temporal difference learning. *CoRR*, abs/2407.04811, 2024.

[35] Luke B. Godfrey. An evaluation of parametric activation functions for deep learning. In *International Conference on Systems, Man and Cybernetics (SMC)*, pages 3006–3011. IEEE, 2019.

[36] Florin Gogianu, Tudor Berariu, Mihaela Rosca, Claudia Clopath, Lucian Busoniu, and Razvan Pascanu. Spectral normalisation for deep reinforcement learning: An optimisation perspective. In *International Conference on Machine Learning (ICML)*, pages 3734–3744, 2021.

[37] Ian J Goodfellow, Mehdi Mirza, Da Xiao, Aaron Courville, and Yoshua Bengio. An empirical investigation of catastrophic forgetting in gradient-based neural networks. *arXiv preprint arXiv:1312.6211*, 2013.

[38] Çaglar Gülçehre, Srivatsan Srinivasan, Jakub Sygnowski, Georg Ostrovski, Mehrdad Farajtabar, Matthew Hoffman, Razvan Pascanu, and Arnaud Doucet. An empirical study of implicit regularization in deep offline RL. *Machine Learning Research*, 2022, 2022.

[39] Tuomas Haarnoja, Aurick Zhou, Pieter Abbeel, and Sergey Levine. Soft actor-critic: Off-policy maximum entropy deep reinforcement learning with a stochastic actor. In *International Conference on Machine Learning (ICML)*, pages 1856–1865, 2018.

[40] Kaiming He, Xiangyu Zhang, Shaoqing Ren, and Jian Sun. Delving deep into rectifiers: Surpassing human-level performance on imagenet classification. In *International Conference on Computer Vision (ICCV)*, pages 1026–1034, 2015.

[41] Kaiming He, Xiangyu Zhang, Shaoqing Ren, and Jian Sun. Deep residual learning for image recognition. In *Conference on Computer Vision and Pattern Recognition (CVPR)*, pages 770–778. IEEE, 2016.

[42] Qiang He, Tianyi Zhou, Meng Fang, and Setareh Maghsudi. Adaptive regularization of representation rank as an implicit constraint of bellman equation. In *International Conference on Learning Representations (ICLR)*, 2024.

[43] Geoffrey E. Hinton, Oriol Vinyals, and Jeffrey Dean. Distilling the knowledge in a neural network. *CoRR*, abs/1503.02531, 2015.

[44] Sepp Hochreiter. The vanishing gradient problem during learning recurrent neural nets and problem solutions. *Int. J. Uncertain. Fuzziness Knowl. Based Syst.*, 6(2): 107–116, 1998.

[45] Sepp Hochreiter and Jürgen Schmidhuber. Flat Minima. *Neural Computation*, 9(1): 1–42, 01 1997. ISSN 0899-7667.

[46] Minyoung Huh, Hossein Mobahi, Richard Zhang, Brian Cheung, Pulkit Agrawal, and Phillip Isola. The low-rank simplicity bias in deep networks. *Trans. Mach. Learn. Res.*, 2023, 2023.

[47] Maximilian Igl, Gregory Farquhar, Jelena Luketina, Wendelin Boehmer, and Shimon Whiteson. Transient non-stationarity and generalisation in deep reinforcement learning. In *International Conference on Learning Representations (ICLR)*. OpenReview.net, 2021.

[48] Leemon C. Baird III. Residual algorithms: Reinforcement learning with function approximation. In Armand Prieditis and Stuart Russell, editors, *International Conference on Machine Learning (ICML)*, pages 30–37. Morgan Kaufmann, 1995.

[49] Ehsan Imani and Martha White. Improving regression performance with distributional losses. In Jennifer G. Dy and Andreas Krause, editors, *International Conference on Machine Learning (ICML)*, volume 80 of *Proceedings of Machine Learning Research*, pages 2162–2171. PMLR, 2018.

[50] Sergey Ioffe and Christian Szegedy. Batch normalization: Accelerating deep network training by reducing internal covariate shift. In Francis R. Bach and David M. Blei, editors, *International Conference on Machine Learning (ICML)*, volume 37 of *JMLR Workshop and Conference Proceedings*, pages 448–456. JMLR.org, 2015.

[51] Tianying Ji, Yongyuan Liang, Yan Zeng, Yu Luo, Guowei Xu, Jiawei Guo, Ruijie Zheng, Furong Huang, Fuchun Sun, and Huazhe Xu. ACE: off-policy actor-critic with causality-aware entropy regularization. In *International Conference on Machine Learning (ICML)*. OpenReview.net, 2024.

[52] Lukasz Kaiser, Mohammad Babaeizadeh, Piotr Milos, Blazej Osinski, Roy H. Campbell, Konrad Czechowski, Dumitru Erhan, Chelsea Finn, Piotr Kozakowski, Sergey Levine, Afroz Mohiuddin, Ryan Sepassi, George Tucker, and Henryk Michalewski. Model based reinforcement learning for atari. In *International Conference on Learning Representations (ICLR)*. OpenReview.net, 2020.

[53] Khimya Khetarpal, Matthew Riemer, Irina Rish, and Doina Precup. Towards continual reinforcement learning: A review and perspectives. *J. Artif. Intell. Res.*, 75: 1401–1476, 2022.

[54] Diederik P. Kingma and Jimmy Ba. Adam: A method for stochastic optimization. In Yoshua Bengio and Yann LeCun, editors, *International Conference on Learning Representations (ICLR)*, 2015.

[55] Aviral Kumar, Aurick Zhou, George Tucker, and Sergey Levine. Conservative q-learning for offline reinforcement learning. In Hugo Larochelle, Marc'Aurelio Ranzato, Raia Hadsell, Maria-Florina Balcan, and Hsuan-Tien Lin, editors, *Advances in Neural Information Processing Systems (NeurIPS)*, 2020.

[56] Aviral Kumar, Rishabh Agarwal, Dibya Ghosh, and Sergey Levine. Implicit underparameterization inhibits data-efficient deep reinforcement learning. In *International Conference on Learning Representations (ICLR)*. OpenReview.net, 2021.

[57] Aviral Kumar, Rishabh Agarwal, Tengyu Ma, Aaron C. Courville, George Tucker, and Sergey Levine. DR3: value-based deep reinforcement learning requires explicit regularization. In *International Conference on Learning Representations (ICLR)*. OpenReview.net, 2022.

[58] Aviral Kumar, Rishabh Agarwal, Xinyang Geng, George Tucker, and Sergey Levine. Offline q-learning on diverse multi-task data both scales and generalizes. In *International Conference on Learning Representations (ICLR)*. OpenReview.net, 2023.

[59] Robert Tjarko Lange. gymnax: A JAX-based reinforcement learning environment library, 2022.

[60] Michael Laskin, Kimin Lee, Adam Stooke, Lerrel Pinto, Pieter Abbeel, and Aravind Srinivas. Reinforcement learning with augmented data. In Hugo Larochelle, Marc'Aurelio Ranzato, Raia Hadsell, Maria-Florina Balcan, and Hsuan-Tien Lin, editors, *Advances in Neural Information Processing Systems (NeurIPS)*, 2020.

[61] Hojoon Lee, Hanseul Cho, Hyunseung Kim, Daehoon Gwak, Joonkee Kim, Jaegul Choo, Se-Young Yun, and Chulhee Yun. PLASTIC: improving input and label plasticity for sample efficient reinforcement learning. In Alice Oh, Tristan Naumann, Amir Globerson, Kate Saenko, Moritz Hardt, and Sergey Levine, editors, *Advances in Neural Information Processing Systems (NeurIPS)*, 2023.

[62] Hojoon Lee, Hyeonseo Cho, Hyunseung Kim, Donghu Kim, Dugki Min, Jaegul Choo, and Clare Lyle. Slow and steady wins the race: Maintaining plasticity with hare and tortoise networks. In *International Conference on Machine Learning (ICML)*. OpenReview.net, 2024.

[63] Alex Lewandowski, Haruto Tanaka, Dale Schuurmans, and Marlos C. Machado. Curvature explains loss of plasticity. *CoRR*, abs/2312.00246, 2023.

[64] Clare Lyle, Mark Rowland, Georg Ostrovski, and Will Dabney. On the effect of auxiliary tasks on representation dynamics. In Arindam Banerjee and Kenji Fukumizu, editors, *International Conference on Artificial Intelligence and Statistics (AISTATS)*, volume 130 of *Proceedings of Machine Learning Research*, pages 1–9. PMLR, 2021.

[65] Clare Lyle, Mark Rowland, and Will Dabney. Understanding and preventing capacity loss in reinforcement learning. In *International Conference on Learning Representations (ICLR)*, 2022.

[66] Clare Lyle, Zeyu Zheng, Evgenii Nikishin, Bernardo Ávila Pires, Razvan Pascanu, and Will Dabney. Understanding plasticity in neural networks. In *International Conference on Machine Learning (ICML)*, volume 202, pages 23190–23211, 2023.

[67] Clare Lyle, Zeyu Zheng, Khimya Khetarpal, James Martens, Hado van Hasselt, Razvan Pascanu, and Will Dabney. Normalization and effective learning rates in reinforcement learning. *CoRR*, abs/2407.01800, 2024.

[68] Clare Lyle, Zeyu Zheng, Khimya Khetarpal, Hado van Hasselt, Razvan Pascanu, James Martens, and Will Dabney. Disentangling the causes of plasticity loss in neural networks. *CoRR*, abs/2402.18762, 2024.

[69] Guozheng Ma, Lu Li, Sen Zhang, Zixuan Liu, Zhen Wang, Yixin Chen, Li Shen, Xueqian Wang, and Dacheng Tao. Revisiting plasticity in visual reinforcement learning: Data, modules and training stages. In *International Conference on Learning Representations (ICLR)*. OpenReview.net, 2024.

[70] Andrew L Maas, Awni Y Hannun, Andrew Y Ng, et al. Rectifier nonlinearities improve neural network acoustic models. In *International Conference on Machine Learning (ICML)*, volume 28 of *JMLR Workshop and Conference Proceedings*. JMLR.org, 2013.

[71] Andrew Kachites McCallum. *Reinforcement learning with selective perception and hidden state.* University of Rochester, 1996.

[72] Michael McCloskey and Neal J Cohen. Catastrophic interference in connectionist networks: The sequential learning problem. In *Psychology of learning and motivation*, volume 24, pages 109–165. Elsevier, 1989.

[73] Edan Meyer, Adam White, and Marlos C. Machado. Harnessing discrete representations for continual reinforcement learning. *CoRR*, abs/2312.01203, 2023.

[74] Takeru Miyato, Toshiki Kataoka, Masanori Koyama, and Yuichi Yoshida. Spectral normalization for generative adversarial networks. In *6th International Conference on Learning Representations, ICLR 2018, Vancouver, BC, Canada, April 30 - May 3, 2018, Conference Track Proceedings.* OpenReview.net, 2018.

[75] Volodymyr Mnih, Koray Kavukcuoglu, David Silver, Andrei A. Rusu, Joel Veness, Marc G. Bellemare, Alex Graves, Martin A. Riedmiller, Andreas Fidjeland, Georg Ostrovski, Stig Petersen, Charles Beattie, Amir Sadik, Ioannis Antonoglou, Helen King, Dharshan Kumaran, Daan Wierstra, Shane Legg, and Demis Hassabis. Human-level control through deep reinforcement learning. *Nat.*, 518(7540):529–533, 2015.

[76] Aditya Mohan, Amy Zhang, and Marius Lindauer. Structure in deep reinforcement learning: A survey and open problems. *J. Artif. Intell. Res.*, 79:1167–1236, 2024.

[77] Kevin P. Murphy. *Probabilistic Machine Learning: An Introduction.* Adaptive Computation and Machine Learning Series. The MIT Press, Cambridge, Massachusetts, 2022. ISBN 978-0-262-04682-4.

[78] Kevin P. Murphy. *Probabilistic Machine Learning: Advanced Topics.* Adaptive Computation and Machine Learning Series. The MIT Press, Cambridge, Massachusetts, 2023. ISBN 978-0-262-04843-9.

[79] Michal Nauman and Marek Cygan. On the theory of risk-aware agents: Bridging actor-critic and economics. In *ICML 2024 Workshop: Aligning Reinforcement Learning Experimentalists and Theorists*, 2023.

[80] Michal Nauman, Michal Bortkiewicz, Piotr Milos, Tomasz Trzcinski, Mateusz Ostaszewski, and Marek Cygan. Overestimation, overfitting, and plasticity in actor-critic: the bitter lesson of reinforcement learning. In *International Conference on Machine Learning (ICML).* OpenReview.net, 2024.

[81] Michal Nauman, Mateusz Ostaszewski, Krzysztof Jankowski, Piotr Milos, and Marek Cygan. Bigger, regularized, optimistic: scaling for compute and sample-efficient continuous control. *CoRR*, abs/2405.16158, 2024.

[82] Evgenii Nikishin, Max Schwarzer, Pierluca D'Oro, Pierre-Luc Bacon, and Aaron C. Courville. The primacy bias in deep reinforcement learning. In Kamalika Chaudhuri, Stefanie Jegelka, Le Song, Csaba Szepesvári, Gang Niu, and Sivan Sabato, editors, *International Conference on Machine Learning (ICML)*, volume 162 of *Proceedings of Machine Learning Research*, pages 16828–16847. PMLR, 2022.

[83] Evgenii Nikishin, Junhyuk Oh, Georg Ostrovski, Clare Lyle, Razvan Pascanu, Will Dabney, and André Barreto. Deep reinforcement learning with plasticity injection. In *Advances in Neural Information Processing Systems (NeurIPS)*, 2023.

[84] Johan S. Obando-Ceron, Marc G. Bellemare, and Pablo Samuel Castro. Small batch deep reinforcement learning. In Alice Oh, Tristan Naumann, Amir Globerson, Kate Saenko, Moritz Hardt, and Sergey Levine, editors, *Advances in Neural Information Processing Systems (NeurIPS)*, 2023.

[85] Johan Samir Obando-Ceron, Aaron C. Courville, and Pablo Samuel Castro. In value-based deep reinforcement learning, a pruned network is a good network. In *International Conference on Machine Learning (ICML)*. OpenReview.net, 2024.

[86] OpenAI, Ilge Akkaya, Marcin Andrychowicz, Maciek Chociej, Mateusz Litwin, Bob McGrew, Arthur Petron, Alex Paino, Matthias Plappert, Glenn Powell, Raphael Ribas, Jonas Schneider, Nikolas Tezak, Jerry Tworek, Peter Welinder, Lilian Weng, Qiming Yuan, Wojciech Zaremba, and Lei Zhang. Solving rubik's cube with a robot hand. *CoRR*, abs/1910.07113, 2019.

[87] Ian Osband, Charles Blundell, Alexander Pritzel, and Benjamin Van Roy. Deep exploration via bootstrapped DQN. In Daniel D. Lee, Masashi Sugiyama, Ulrike von Luxburg, Isabelle Guyon, and Roman Garnett, editors, *Advances in Neural Information Processing Systems 29 (NeurIPS)*, pages 4026–4034, 2016.

[88] Georg Ostrovski, Marc G. Bellemare, Aäron van den Oord, and Rémi Munos. Count-based exploration with neural density models. In Doina Precup and Yee Whye Teh, editors, *International Conference on Machine Learning (ICML)*, volume 70 of *Proceedings of Machine Learning Research*, pages 2721–2730. PMLR, 2017.

[89] Georg Ostrovski, Pablo Samuel Castro, and Will Dabney. The difficulty of passive learning in deep reinforcement learning. In Marc'Aurelio Ranzato, Alina Beygelzimer, Yann N. Dauphin, Percy Liang, and Jennifer Wortman Vaughan, editors, *Advances in Neural Information Processing Systems 34 (NeurIPS)*, pages 23283–23295, 2021.

[90] Adam Paszke, Sam Gross, Francisco Massa, Adam Lerer, James Bradbury, Gregory Chanan, Trevor Killeen, Zeming Lin, Natalia Gimelshein, Luca Antiga, Alban Desmaison, Andreas Köpf, Edward Z. Yang, Zachary DeVito, Martin Raison, Alykhan Tejani, Sasank Chilamkurthy, Benoit Steiner, Lu Fang, Junjie Bai, and Soumith Chintala. Pytorch: An imperative style, high-performance deep learning library. In Hanna M. Wallach, Hugo Larochelle, Alina Beygelzimer, Florence d'Alché-Buc, Emily B. Fox, and Roman Garnett, editors, *Advances in Neural Information Processing Systems 32 (NeurIPS)*, pages 8024–8035, 2019.

[91] Eduardo Pignatelli, Johan Ferret, Matthieu Geist, Thomas Mesnard, Hado van Hasselt, and Laura Toni. A survey of temporal credit assignment in deep reinforcement learning. *Trans. Mach. Learn. Res.*, 2024, 2024.

[92] Tom Schaul, André Barreto, John Quan, and Georg Ostrovski. The phenomenon of policy churn. In Sanmi Koyejo, S. Mohamed, A. Agarwal, Danielle Belgrave, K. Cho,

and A. Oh, editors, *Advances in Neural Information Processing Systems (NeurIPS)*, 2022.

[93] Julian Schrittwieser, Ioannis Antonoglou, Thomas Hubert, Karen Simonyan, Laurent Sifre, Simon Schmitt, Arthur Guez, Edward Lockhart, Demis Hassabis, Thore Graepel, Timothy P. Lillicrap, and David Silver. Mastering atari, go, chess and shogi by planning with a learned model. *Nat.*, 588(7839):604–609, 2020.

[94] Max Schwarzer, Johan Samir Obando-Ceron, Aaron C. Courville, Marc G. Bellemare, Rishabh Agarwal, and Pablo Samuel Castro. Bigger, better, faster: Human-level atari with human-level efficiency. In Andreas Krause, Emma Brunskill, Kyunghyun Cho, Barbara Engelhardt, Sivan Sabato, and Jonathan Scarlett, editors, *International Conference on Machine Learning (ICML)*, volume 202 of *Proceedings of Machine Learning Research*, pages 30365–30380. PMLR, 2023.

[95] Wenling Shang, Kihyuk Sohn, Diogo Almeida, and Honglak Lee. Understanding and improving convolutional neural networks via concatenated rectified linear units. In Maria-Florina Balcan and Kilian Q. Weinberger, editors, *International Conference on Machine Learning (ICML)*, volume 48 of *JMLR Workshop and Conference Proceedings*, pages 2217–2225. JMLR.org, 2016.

[96] David Silver, Aja Huang, Chris J. Maddison, Arthur Guez, Laurent Sifre, George van den Driessche, Julian Schrittwieser, Ioannis Antonoglou, Vedavyas Panneershelvam, Marc Lanctot, Sander Dieleman, Dominik Grewe, John Nham, Nal Kalchbrenner, Ilya Sutskever, Timothy P. Lillicrap, Madeleine Leach, Koray Kavukcuoglu, Thore Graepel, and Demis Hassabis. Mastering the game of go with deep neural networks and tree search. *Nat.*, 529(7587):484–489, 2016.

[97] Ghada Sokar, Rishabh Agarwal, Pablo Samuel Castro, and Utku Evci. The dormant neuron phenomenon in deep reinforcement learning. In Andreas Krause, Emma Brunskill, Kyunghyun Cho, Barbara Engelhardt, Sivan Sabato, and Jonathan Scarlett, editors, *International Conference on Machine Learning (ICML)*, volume 202 of *Proceedings of Machine Learning Research*, pages 32145–32168. PMLR, 2023.

[98] Richard S. Sutton and Andrew G. Barto. *Reinforcement learning - an introduction.* Adaptive computation and machine learning. MIT Press, 1998. ISBN 978-0-262-19398-6.

[99] Yuval Tassa, Yotam Doron, Alistair Muldal, Tom Erez, Yazhe Li, Diego de Las Casas, David Budden, Abbas Abdolmaleki, Josh Merel, Andrew Lefrancq, Timothy P. Lillicrap, and Martin A. Riedmiller. Deepmind control suite. *CoRR*, abs/1801.00690, 2018.

[100] Emanuel Todorov, Tom Erez, and Yuval Tassa. Mujoco: A physics engine for model-based control. In *2012 IEEE/RSJ International Conference on Intelligent Robots and Systems, IROS 2012, Vilamoura, Algarve, Portugal, October 7-12, 2012*, pages 5026–5033. IEEE, 2012.

[101] Aäron van den Oord, Oriol Vinyals, and Koray Kavukcuoglu. Neural discrete representation learning. In Isabelle Guyon, Ulrike von Luxburg, Samy Bengio, Hanna M. Wallach, Rob Fergus, S. V. N. Vishwanathan, and Roman Garnett, editors, *Advances in Neural Information Processing Systems 30: Annual Conference on Neural Information Processing Systems 2017, December 4-9, 2017, Long Beach, CA, USA*, pages 6306–6315, 2017.

[102] Hado van Hasselt. Double q-learning. In John D. Lafferty, Christopher K. I. Williams, John Shawe-Taylor, Richard S. Zemel, and Aron Culotta, editors, *Advances in Neural Information Processing Systems (NeurIPS)*, pages 2613–2621. Curran Associates, Inc., 2010.

[103] Hado van Hasselt, Yotam Doron, Florian Strub, Matteo Hessel, Nicolas Sonnerat, and Joseph Modayil. Deep reinforcement learning and the deadly triad. *CoRR*, abs/1812.02648, 2018.

[104] Liyuan Wang, Xingxing Zhang, Hang Su, and Jun Zhu. A comprehensive survey of continual learning: Theory, method and application. *IEEE Trans. Pattern Anal. Mach. Intell.*, 46(8):5362–5383, 2024.

[105] Xu Wang, Sen Wang, Xingxing Liang, Dawei Zhao, Jincai Huang, Xin Xu, Bin Dai, and Qiguang Miao. Deep reinforcement learning: A survey. *IEEE Trans. Neural Networks Learn. Syst.*, 35(4):5064–5078, 2024.

[106] Tongtong Wu, Linhao Luo, Yuan-Fang Li, Shirui Pan, Thuy-Trang Vu, and Gholamreza Haffari. Continual learning for large language models: A survey. *CoRR*, abs/2402.01364, 2024.

[107] Guowei Xu, Ruijie Zheng, Yongyuan Liang, Xiyao Wang, Zhecheng Yuan, Tianying Ji, Yu Luo, Xiaoyu Liu, Jiaxin Yuan, Pu Hua, Shuzhen Li, Yanjie Ze, Hal Daumé III, Furong Huang, and Huazhe Xu. Drm: Mastering visual reinforcement learning through dormant ratio minimization. In *International Conference on Learning Representations (ICLR)*. OpenReview.net, 2024.

[108] Jingjing Xu, Xu Sun, Zhiyuan Zhang, Guangxiang Zhao, and Junyang Lin. Understanding and improving layer normalization. In Hanna M. Wallach, Hugo Larochelle, Alina Beygelzimer, Florence d'Alché-Buc, Emily B. Fox, and Roman Garnett, editors, *Advances in Neural Information Processing Systems 32 (NeurIPS)*, pages 4383–4393, 2019.

[109] Denis Yarats, Ilya Kostrikov, and Rob Fergus. Image augmentation is all you need: Regularizing deep reinforcement learning from pixels. In *International Conference on Learning Representations (ICLR)*. OpenReview.net, 2021.

[110] Denis Yarats, Rob Fergus, Alessandro Lazaric, and Lerrel Pinto. Mastering visual continuous control: Improved data-augmented reinforcement learning. In *International Conference on Learning Representations (ICLR)*. OpenReview.net, 2022.

[111] Tianhe Yu, Deirdre Quillen, Zhanpeng He, Ryan Julian, Karol Hausman, Chelsea Finn, and Sergey Levine. Meta-world: A benchmark and evaluation for multi-task and meta reinforcement learning. In Leslie Pack Kaelbling, Danica Kragic, and Komei Sugiura, editors, *Conference on Robot Learning (CoRL)*, volume 100 of *Proceedings of Machine Learning Research*, pages 1094–1100. PMLR, 2019.

[112] Da-Wei Zhou, Hai-Long Sun, Jingyi Ning, Han-Jia Ye, and De-Chuan Zhan. Continual learning with pre-trained models: A survey. In *Joint Conference on Artificial Intelligence (IJCAI)*, pages 8363–8371. ijcai.org, 2024.